A systematic appraisal of the Eriophyoidea (Acari: Prostigmata)

by

Charnie Craemer

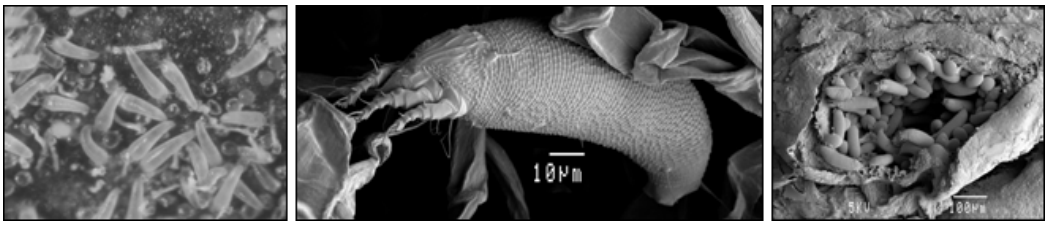

Submitted in partial fulfilment of the requirements for the degree

Philosophiae Doctor in Zoology

In the

Faculty of Natural & Agricultural Sciences

University of Pretoria

Pretoria

South Africa

Supervisors: Profs. Clarke H. Scholtz and Christian T. Chimimba

NOVEMBER 2010

A systematic appraisal of the Eriophyoidea (Acari: Prostigmata)

by

Charnie Craemer*

Supervisors: Prof C.H. Scholtz
Scarab Research Group
Department of Zoology and Entomology
University of Pretoria
Pretoria
0002 South Africa
E-mail: chscholtz@zoology.up.ac.za

Prof C.T. Chimimba
DST-NRF Centre of Excellence for Invasion Biology (CIB) &
Mammal Research Institute (MRI)
Department of Zoology and Entomology
University of Pretoria
Pretoria
0002 South Africa
E-mail: ctchimimba@zoology.up.ac.za

*Present address: Biosystematics Division
Agricultural Research Council – Plant Protection Research Institute
Private Bag X134
Pretoria, Queenswood
0121 South Africa
E-mail: craemerc@arc.agric.za or charnie@telkomsa.net

Declaration

I, Charnie Craemer, declare that the thesis/dissertation, which I hereby submit for the degree Philosophiae Doctor in Zoology at the University of Pretoria, is my own work and has not previously been submitted by me for a degree at this or any other tertiary institution.

SIGNATURE……

DATE……...

Abstract

The diversity of the Eriophyoidea is largely unknown and their systematic study mostly entails alpha-taxonomy which is critically important for these mites. Eriophyoid morphology is almost exclusively studied on slide-mounted specimens, and truly permanent specimen slides cannot be prepared and are eventually lost. Shortcomings in taxon descriptions are persistent, and too few morphological characters are available for systematic use, particularly for phylogenetic studies. The fragile, simplified and minute eriophyoid bodies, and the inadequacy of study methods and technology, including preparation and light microscopy, contribute to these problems. The present eriophyoid classification is widely accepted, relatively stable and useful. The major part of the classification, however, is probably artificial, and some taxon delimitations and identifications are becoming increasingly difficult.

Scanning electron microscopy (SEM) is only sporadically used to supplement conventional descriptions of eriophyoid mites, and their phylogeny has hardly been studied. In the present study some aspects of eriophyoid systematics and its improvements by incorporating SEM for morphological study and phylogenetic analyses for testing and improving the naturalness of the present eriophyoid classification, are used and appraised.

The morphology of about 64 species, mostly from South Africa, was studied with low-temperature (cryo) SEM. The specimens remained turgid and the shape of the mites largely unaltered. A general overview of the contribution of the SEM study towards systematic morphology of the Eriophyoidea is presented. Discrepancies between species descriptions from slide-mounted specimens and the SEM images were found. These include body form, interpretation of structures, resolution and information on minute morphology, and the presence of secretions. Some of these differences were caused by artefacts introduced with slide-mounting of specimens. The SEM study includes a comparative morphological study of the gnathosoma, including a review and appraisal of characters presently used in eriophyoid systematics. New morphological information was found, including new characters that may be of systematic use. Morphology studied with SEM should be routinely incorporated into eriophyoid descriptions, which is not presently the case.

The phylogeny of the Eriophyoidea was studied at genus level, using morphological data, to test the monophyly of the present suprageneric taxa. Three data matrices with 66, 60 and 27 informative characters of 316 (including most *Diptilomiopus* spp.), 64 and 17 eriophyoid ingroup species respectively were analyzed with parsimony analyses, and trees were searched under different parameters. This was done to find different hypotheses regarding the taxon relationships, to roughly assess the robustness of the tree groups, and to use different approaches: a very comprehensive taxon sample, but with low ratio of characters to taxa; an exemplar species sample

to improve the ratio between characters to taxa; and a very small taxon sample with a good ratio between characters and taxa, but very little inclusion of variation found in the Eriophyoidea. Most groups found were supported only by homoplasy, but many made biological sense and various potentially monophyletic groups, additional to taxa in the present classification, are proposed for further study. The robustness and convergence of these groups on monophyly are discussed. The Phytoptidae was found to be polyphyletic. Part of the Nalepellinae is probably positioned outside the remainder of the Eriophyoidea, while the rest of the Phytoptidae were positioned in smaller subgroups among the Eriophyidae. The Phytoptinae and Sierraphytoptinae, including *Pentasetacus*, may group together. The Eriophyidae never grouped together with much support, and the family is both polyphyletic and paraphyletic. The Diptilomiopidae was largely found to be monophyletic, with a relatively strong phylogenetic structure. The Rhyncaphytoptinae is mainly paraphyletic, and the Diptilomiopinae polyphyletic, but part of the Diptilomiopinae may be monophyletic.

Three new *Diptilomiopus* spp. from South Africa are described as part of the study: *D. faurius* sp. nov. from *Faurea rochetiana* (A. Rich.) Pic. Serm. (Proteaceae); D. *apobrevus* sp. nov. and *D. apolongus* sp. nov. from *Apodytes dimidiata* E. Mey. ex Arn. (Icacinaceae). They were leaf vagrants not causing any observable symptoms.

Key words: Acari, Eriophyoidea, Eriophyidae, Phytoptidae, Diptilomiopidae, systematics, mites, eriophyoid mites, taxonomy, classification, phylogeny, morphology, gnathosoma, worldwide, scanning electron microscopy, SEM, *Diptilomiopus*, new combinations, new species, South Africa

DEDICATION

This dissertation is dedicated to Professor Valeriy Shevchenko (1929 – 2010)[1]

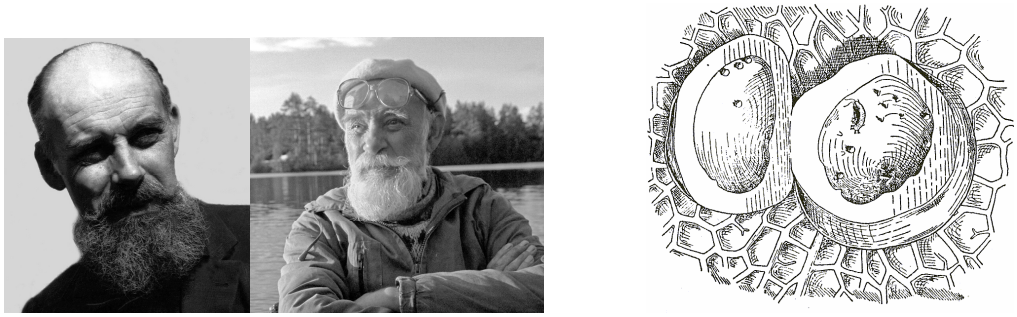

Prof. Valeriy Shevchenko (two photos on left), and a line drawing of an *Eriophyes laevis* colony inside a gall (right), and the "birth" of *E. laevis* (below) (from Shevchenko, 1961). The drawings were scanned from badly photocopied drawings, and the reproductions are not good, but they illustrate Shevchenko's attention to detail.

Valeriy Shevchenko was born on 3 October 1929, in Vladivostok, in the Far East of Russia, but grew up in Leningrad (today St. Petersburg), where he essentially spent his whole life. During his university studies, he chose as his research subject, the then largely unexplored Eriophyoidea (his "Tetrapodili"), and presented the morphology of alder gall mite, *Eriophyes laevis*, for a PhD-degree. Thus began his life-long dedication to the study of these mites at Leningrad State University. He is regarded as the founder of the Russian school of Eriophyoidology.

His research largely concentrated on mite pests of junipers. Early in his career he undertook an expedition into the mountain districts of the Kyrgyz Republic in order to advise the forestry specialists on methods of controlling eriophyoid injury to cultivated juniper trees. He subsequently spent many seasons in these regions, studying the biology and morphology of eriophyoid mites and methods of controlling them. He fell in love with the picturesque nature of central Asia, especially with the mountain forests which are now threatened, exploring it up to the end of his life. He studied different aspects of the evolution of the Eriophyoidea, and his favorite subjects of inquiry remained the Nalepellinae, which live on coniferous trees, and which he believed are the key to understanding eriophyoid evolution. He insisted Eriophyoidea evolution should be examined alongside the evolution of their host-plants. His publications are frequently referred to in the chapter on phylogeny in the present dissertation.

His research on, and his insight in the evolution and phylogeny of the Eriophyoidea prompted me to contact him several years ago. During our ongoing e-mail communication I learned to love and respect him. I found him a fascinating and kind person. Although he dedicated his life to the study of his beloved "four-legged mites", his talents and interests included drawing, public speaking and writing poetry and novels. He also wrote a novel about his famous grandfather "Viktor Vologdin, the welder", and he had a keen interest in Russian politics, and the decline of the Asian forests. We unfortunately seldom discussed the phylogeny of the Eriophyoidea, though, because we planned for me to visit him. Due to my workload and the necessity to first finish my PhD studies, the visit never realized. It was with shock that I learned of his death, at the age of 80, on 22 March 2010, with the sickening realization that I will never have the privilege to meet him in person and discuss the phylogeny of the Eriophyoidea with him. I dedicate this dissertation to him and thank him for his contribution to enriching my life.

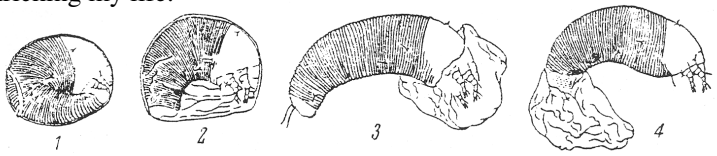

[1] Some information in this dedication is from Sukhareva & Chetverikov (2010).

ACKNOWLEDGEMENTS

First, I thank my promoters, **Profs. Clarke Scholtz** and **Chris Chimimba**, for accommodating me as their student, and their support and patience even when the study became long overdue. Thanks also for their noteworthy improvements of the final versions of the dissertation. Sincere thanks to **Prof. Ansie Dippenaar-Schoeman** for her endless encouragement and support. She helped me to commence the study, and finish it, and improved some parts of the dissertation. Without her back up at work and during difficult periods, and moments of crises, it would not have been possible. I cannot have a better role model to follow for becoming an outstanding and productive scientist. *Dankie, Ansie*! Thanks to **Prof. Eddie Ueckermann**, my mite colleague, who is the kindest person I know, and who took over the responsibility for some of the plant-feeding mite groups, to allow me to concentrate on the Eriophyoidea. He also assisted me in choosing the outgroup species and naming their structures.

Thanks to **Prof. Stefan Neser**, an amazing scientist and naturalist, who put me on the path of studying the Eriophyoidea. Without him, any significant biosystematic research on the Eriophyoidea in South Africa probably would not have commenced, and most of the research on these mites in this country is based on material he collected, including most of the specimens used in the present study.

Special thanks to **Alan Hall** who assisted me throughout the SEM study, and who prepared and set up the microscope and specimens for each session. Without him, the results of the SEM study would not have attained the quality it did. He improved some of the procedures, and went to utmost trouble to ensure that we got the best from each session, despite the antics of the microscope. He took real interest in the study, and went far beyond his duty, sometimes with personal sacrifices, in keeping the facility working and to my disposal even to late in the evenings. It was a pleasure to work with him. He also improved the Materials and Methods concerning the SEM study in this dissertation.

My gratitude to **Dr. Pablo Goloboff** for the workshop he presented in South Africa on using TNT, and the insight I gained from his lectures in several aspects of phylogeny. The phylogenetic analyses in the present study were not possible in any other program, and without TNT, this part of the study would not have had usable results. Thanks also to Dr. Goloboff for assistance with some problems I encountered in the program. Thanks to **Prof. Tim Crowe** who initiated and organized this workshop, and to the South African Biosystematics Initiative of the National Research Foundation of South Africa who funded it. Thanks also to **Dr. Steve Farris**, one of the "fathers" of cladistics who co-presented the workshop. Meeting him will always remain an inspiration.

Professional and personal thanks to **Dawid Swart**, my husband. It is well known that one's close family sacrifices much during a doctorate study. Dawid did not just endure this with staying power and with nonstop support; he gives me extraordinary space to lead my own life and follow

my career and enabled my finishing this study. He also spent many hours in editing and improving this dissertation, and checking endless details. *Baie dankie, Dawid*!

I thank the **University of Pretoria** for financial assistance with some of my registration and course fees, and for the use of their infrastructure, in particular the SEM facilities; the **Department of Zoology and Entomology** of this university for allowing me to register for the degree; and the **Agricultural Research Council – Plant Protection Research Institute** (ARC–PPRI) who allowed me to combine some of the research at work with the research towards partial fulfilment of this degree.

My sincere gratitude to my overseas colleagues for their support and assistance, and for their friendship:

- **Prof. Jim W. Amrine jr**, of the University of West Virginia, USA, who, despite his overwhelming work load always answered my questions, of which the *personal communications* attributed to him in this dissertation attest.
- The late **Prof. Valeryi Shevchenko** for continuous e-mail communication (also see dedication above).
- **Prof. Enrico de Lillo** of the University of Bari, Italy, who evaluated an early draft of Chapter 3 (the SEM study) and gave me invaluable advise about my reasoning and interpretation of results, and for his special friendship.
- **Dr. Ron Ochoa** of the USDA, Beltsville, USA, for inviting me to visit him during the study, during which he, among other guidance, exposed me to his phylogenetic research on mites, including his preliminary analyses of the Phytoptidae (see Chapter 4). He also edited an early draft of the phylogenetic results regarding the Phytoptidae. His enthusiasm and love for mites, and nonstop energy, is an inspiration.
- **Prof. Angie Chandrapatya** who edited an early draft of an annotated species list of *Diptilomiopus* who never made it into the final dissertation, and for lending me specimens of *Diptilomiopus* spp. she described, and also thanks to **Dr. K.-W Huang** for the *Diptilomiopus* specimens I borrowed from him.
- **Dr. Mariam Lekveishvili** for giving me information about her molecular study on the Eriophyoidea.
- **Dr. Evert Lindquist** for warning me about testing for birefringence before a structure can be considered a seta.
- Also thanks to **Drs. Sebahat Ozman Sullivan, C.H.W. Flechtmann, Denise Navia, Anna Skoracka, Brian Fenton, Carl Childers, Danuta Knihinicki, Eric Palevsky, Tom Morley**, in no order of importance.

My sincere thanks to my colleagues particularly at ARC-PPRI, and elsewhere in South Africa, for their support and interest in the study, and for their friendship:

- **Riaan Stals** for his valuable discussions on systematics and particularly phylogeny and for his advise which always taught me something. He also provided me with some core cladistic articles. He is a never-ending source of knowledge, and his enthusiasm for science is an inspiration.
- **Beatrix Sunkel**, **Lindie Steynberg** and **Tshidi Makutoane** for general assistance throughout the years.
- **Johan Coetzer** who assisted me in getting the best computer facilities he could, got an extra computer for me to ran the analyses, and who always goes out of his way to help with any computer problems, far beyond his duty.
- **Dr. Riana Jacobs** who gave me information about PAUP and her view on phylogeny using molecular data.
- **Dr. Connal Eardley** for sound taxonomic advice and for prompting me to translate the phylogenetic results into a formally proposed classification.
- **Hannetjie Combrink** and **Louise Coetzee** of the library who found many obscure articles for me**.**
- **Elsa van Niekerk** for the design of the dissertation cover, and assistance with printing the dissertation.
- **Dr. Antoinette Swart** for reviewing the "alpha and omega" (the first drafts of the Introduction and General Conclusions).
- The late **Dr. Lenie Meyer,** who believed that I will be able to become an acarologist.
- Also thanks to **Profs. Pieter Theron** and **Stefan Foord; Drs. Isabel Rong, Roger Price, Esther v.d. Berg, Lorenco Prendini**, **Mariette Marais** and **Tonie Putter**; and **Hildegard Klein, Liamé v.d. Westhuizen, Marika v.d. Merwe, Annette v.d. Berg, Connie Anderson, Naomi Buckley** and **Allet Lewis**.

On a personal note, I thank my mother, **Henriëtte Craemer**, who is a constant source of support and love in my life. She frequently asked whether it is worthwhile to continue with something that is causing me so much stress, which actually helped to strengthen my resolve to finish it. Also thanks to my aunt, Sallaum, for her interest, and particularly in when I am going to finish. Special thanks to Drs. Engela Young, Adéle Potgieter, and to Isabel Botha, and two horses, Mona and Wyn.

Finally yet importantly, thanks to all the researchers who spent endless hours in describing these smallest of mites. Without their data, this study would not have been possible.

DISSERTATION OUTLINE AND CONTENT

Prologue: A brief introduction to the Acari including classification of the Acari, and biology and ecology of the Eriophyoidea.

Chapter 1: Aims, scope and approaches of this study, followed by a brief review of the evolution, diversity and systematics of the Eriophyoidea.

Chapter 2: General material and methods. A relational database with descriptive data captured from published descriptions, including 304 species records and 400 descriptive fields each, has been prepared to provide data for the present study. In particular, electronic procedures, formats and programs for capturing and structuring descriptive data are proposed and discussed.

Chapter 3: A systematic morphological study of the Eriophyoidea utilizing low-temperature scanning electron microscopy (LT-SEM). It includes an appraisal of some of the characters and character states used in eriophyoid systematics, with emphasis on artefacts caused by slide-mounting; and additional information from SEM studies. The morphology of *ca.* 64 species from South Africa was studied, and includes a comparative morphological study of the gnathosoma based on SEM study. Characters which have not previously been used for eriophyoid systematics are described and their potential systematic usefulness is appraised.

Chapter 4: Phylogenetic parsimony analyses of the Eriophyoidea under different parameters to study relationships between mostly type species of genera worldwide, and to test monophyly of suprageneric groups. Monophyly of suprageneric groupings are appraised and hypothetically monophyletic groups within the Eriophyoidea are identified and proposed for further study.

Chapter 5: General conclusions.

Apart from other Appendices: An article describing three new *Diptilomiopus* spp. from South Africa, which will be submitted to *Systematics and Biodiversity*, is included (Appendix M).

TABLE OF CONTENTS

CHAPTER 2: GENERAL MATERIAL AND METHODS

CHAPTER 3: MORPHOLOGY AND SYSTEMATICS

APPENDICES

Appendix A. Alphabetic list of species included in the phylogenetic analyses.

Appendix B. Characters coded for phylogenetic analyses: definition, description and discussion.

Appendix C. Character numbers of characters in all analyses.

Appendix D. Data matrix for 318-taxon analyses.

Appendix E. Abbreviated character definition for 66-taxon analyses.

Appendix F. Data matrix for 66-taxon analyses.

Appendix G. **G.1.** Character definition for 18-taxon original and corrected analyses.

G.2. Character definition for 18-taxon modified analyses.

Appendix H. **H.1.** Original data matrix (Hong & Zhang, 1996a) for 18-taxon analyses.

H.2. Corrected data matrix for 18-taxon analyses.

H.3. Modified data matrix for 18-taxon analyses.

Appendix I. Glossary.

Appendix J. Published abstracts 1 & 2.

J.1. Craemer, C. & Hall, A.N. 2003. The use of low-temperature scanning electron microscopy for studying eriophyoid mites (Acari: Eriophyoidea). p. 76 In: *Proceedings of the Microscopy Society of Southern Africa* 33.

J.2. Craemer, C. 2006. Morphology of eriophyoid mites (Eriophyoidea) as elucidated by scanning electron microscopy: trivial pursuit or valuable systematic contribution? p. 45 In: Bruin, J. (Ed.). *Abstract Book.* 12th International Congress of Acarology, 21-26 August 2006, Amsterdam, The Netherlands.

Appendix K. Published article 3.

Craemer, C.; Amrine, J.W. Jr.; De Lillo, E. & Stasny, T.A. 2005. Nomenclatural changes and new synonymy in the genus *Diptilomiopus* Nalepa, 1916 (Acari: Eriophyoidea: Diptilomiopidae). *International Journal of Acarology* 31: 133–136.

Appendix L. Published article 4.

De Lillo, E.; Craemer, C.; Amrine, J.W. Jr. & Nuzzaci, G. 2010. Recommended procedures and techniques for morphological studies of Eriophyoidea (Acari: Prostigmata). *Experimental and Applied Acarology* 51: 283–307. DOI 10.1007/s10493-009-9311-x

Appendix M. Submitted article 5.

Craemer, C. 2010. Description of three new *Diptilomiopus* spp. (Eriophyoidea: Diptilomiopidae) from South Africa. (will be submitted to *Systematics and Biodiversity*)

LIST OF FIGURES

PROLOGUE

CHAPTER 3

Except where otherwise indicated, all figures in chapter 3 are SEM images.

Trisetacus cupressi Keifer, 1944, drawings by H.H. Keifer, reproduced from Keifer (1944): **h)** internal genitalia (modified from Keifer, 1944), **i)** coxi-genital area. All reproductions with permission where necessary.

Fig. 3.6. Legs and leg structures of adult eriophyoid females. Legs of *Aculops rhodensis* (Keifer, 1957) as drawn by E. de Lillo, from De Lillo (1988): **a)** leg I; **b)** leg II. Different shapes of eriophyoid empodia (featherclaws) of various species: **c)** *Cecidophyes rouhollahi*, drawing by C. Craemer (reproduced from Craemer *et al*., 1999); **d)** *C. rouhollahi*, drawing by H.H. Keifer (reproduced from Craemer *et al*., 1999); **e)** *Dicrothrix anacardii* Keifer, 1966 (reproduced from Keifer, 1966b); **f)** *Dechela epelis* Keifer, 1965 (modified from Keifer, 1965a); **g)** *Acaphyllisa parindiae* Keifer, 1978 (reproduced from Keifer, 1978); **h)** *Diptilomiopus faurius* sp. nov. (Appendix L); **i)** *Acarhis lepisanthis* Keifer, 1975 (reproduced from Keifer, 1975d); **j)** *Acarhynchus filamentus* Keifer, 1959 (reproduced from Keifer, 1959b); **k)** *Diptiloplatus megagrastis* Keifer, 1975 (reproduced from Keifer, 1975c); **l)** *Acritonotus denmarki* Keifer, 1962 (reproduced from Keifer, 1962b); **m)** *Brevulacus reticulatus* Manson, 1984, protogyne female (modified from Manson, 1984a); **n**) *Aberoptus samoae* Keifer, 1951, leg I (modified from Keifer, 1951).

Fig. 3.7. Unmodified SEM images: **a)** Specimens of *Cecidodectes euzonus* Nalepa, 1917 among erineum hairs caused by them on *Trema orientalis*, illustrating the difficulty to sometimes find the mites within complicated plant structures when viewed in a SEM. This and the need to view them from different aspects, creates the need to mount them individually for systematic purposes; **b)** Individual of *Aberoptus*, probably new species, *in situ* on a *Schotia brachypetala* leave - note the good turgor, with no apparent shape distortion, of both plant and mite material, including mite eggs; **c**) *Tergilatus sparsus* Meyer & Ueckermann, 1995 on *Portulacaria afra* – a piece of plant material (leave in this case) with live mites *in situ*, mounted on adhesive carbon tape; **d)** individual mites of *Meyerella bicristatus* (Meyer, 1989) from *Mystroxylon aethiopicum* stuck onto adhesive carbon tape to facilitate observation of different aspects of the mite specimens.

Fig. 3.8. (continued on next page) Dorsal views of legs of: **a)** *Trisetacus* sp. (Phytoptidae: Nalepellinae: Trisetacini), bud mite on *Pinus pinaster*; **b)** *Diptilomiopus faurius* sp. nov. (Diptilomiopidae: Diptilomiopinae), leaf vagrant on *Faurea rochetiana*; **c)** *Cecidophyopsis* sp. (Eriophyidae: Cecidophyinae: Cecidophyini), leaf vagrant on *Yucca guatemalensis*, **d)** *Afromerus* sp. (Eriophyidae: Cecidophyinae: Colomerini), leaf galls on *Psydrax livida*, (the fine cracks are artificial, caused by deterioration of specimen in SEM); **e)** unknown family (Eriophyoidea), vagrant on green fruit of *Anthocleista grandiflora*. Solid white arrows: dorsal completeness of margin between femur and genu on leg I, and presence, position and number of spines on this margin; solid black arrows: ornamentation on femur of leg I; open arrows: shape of tibia of leg I.

Fig. 3.8. (continued from previous page) **f, g)** *Aculus* sp. (Eriophyidae: Phyllocoptinae: Anthocoptini), vagrant on *Lantana trifolia*; **h)** leg I and **i)** leg II of *cf. Calacarus* sp. (Eriophyidae: Phyllocoptinae: Calacarini), leaf vagrant on *Psydrax livida*; **j)** *Acalitus mallyi* (Eriophyidae: Eriophyinae: Aceriini), leaf galls on *Vangueria infausta* subsp. *infausta*; **k)** *cf. Aceria* sp. (Eriophyidae: Eriophyinae: Aceriini), leaf galls on *Acacia rehmanniana*; **l)** *Aceria* sp. (Eriophyidae: Eriophyinae: Aceriini), erineum and distortion on *Ipomoea batatas* var. *batatas*. Solid white arrows: dorsal completeness of margin between femur and genu on leg I, and presence, position and number of spines on this margin; solid black arrows: ornamentation on femur of leg I; open arrows: shape of tibia on leg I; white triangles: segment margins on which spicules are present.

Fig. 3.9. *Diptilomiopus faurius* sp. nov. from *Faurea rochetiana* (Appendix L), ventral view of leg I, with a pattern of ridges, **a)** clearly visible in the SEM images, but, **b)** barely visible in the slide-mounted specimens. This descriptive drawing was drawn from the specimen with the most complete visibility of these ridges.

Fig. 3.10. Empodium on tarsus of leg I of *Diptilomiopus faurius* sp. nov. (Appendix L) from *Faurea rochetiana*: **a)** dorsal view depicting shape, **b)** lateral view facilitating count of rays – the empodium of this species has eight rays.

Fig. 3.11. Distal parts of tarsi with focus on the empodia: **a)** *Trisetacus* sp. from *Pinus pinaster*; **b)** *Cecidophyopsis* sp. from *Yucca guatemalensis*; **c)** *Shevtchenkella* sp. from *Psydrax livida*; **d)** unknown species from *Dovyalis*; **e)** unknown species from *Faurea rochetiana*; **f)** *Acalitus mallyi*; **g)** *Aceria* sp. from *Ipomoea batatas*; **h)** unknown species from *Apodytes dimidiata*.

Fig. 3.12. External female genitalia of *Tergilatus sparsus* Meyer & Ueckermann, 1995 (Meyer & Ueckermann, 1995): **a)** slide-mounted specimen (holotype) viewed with phase contrast; **b)** drawing made from slide-mounted specimen; **c)** SEM image of same area in another specimen. Drawing reproduced from the original unpublished drawing with permission from the authors.

Fig. 3.13. Ambulacra with tenent hairs: **a)** leg II of an *Aponychus* sp. (Tetranychidae) from *Solanum mauritianum*; **b)** leg I of a species of the Tenuipalpidae from a *Senecio* sp.; **c)** leg I of a species of the Stigmaeidae from *Apodytes dimidiata*. Empodia with slightly knobbed hairs or rays (*Tydeus*) and "tenent" hairs or rays (*Aberoptus*) of: **d)** leg I of *cf. Tydeus* sp. (Tydeidae) from *Ekebergia capensis* Sparrm.; **e, f)** leg II of an *Aberoptus* sp. (Eriophyidae) from *Schotia brachypetala*; **a, c, f)** scale lines = 10 µm; **b, d, e)** scales line = 1 µm. Arrows pointing towards tips of hairs of rays, with an enlarged drawing of the tip of the ray of the empodium of the *Aberoptus* sp. in image 3.13f.

Fig. 3.14. Microtubercles of *Aceria* sp. nov. from *Ipomoea batatas*: dorsally on first annuli behind the prodorsal shield rear margin - **a, b)** SEM images, **d)** line drawing; dorsally on rear caudal annuli - **c)** SEM image, **f)** line drawing; on ventral annuli about between setae e - **g)** line drawing, **h)** SEM image; on rear, caudal ventral annuli - **e)** line drawing, **i)** SEM image; all scale lines = 10 µm except **h)** scale line = 1 µm.

Fig. 3.15. *Meyerella bicristatus* (Meyer, 1989b), leaf vagrant on *Mystroxylon aethiopicum* subsp. *aethiopicum*: **a)** SEM image of dorso-lateral aspect (scale line = 10 µm); **b)** part of slide-mounted specimens (female) viewed with phase contrast light microscopy in lateral view; **c)** line drawing (reproduced from the original drawing by Meyer with permission) of the specimen digitally imaged in 3.15b. Arrows indicating: ribs or striae on lobes in SEM image; striae very vaguely present in this one slide-mounted specimen of a series of about 100 specimens in which they were invisible (the lines are hardly visible in the printed copy, but when this image is enlarged on screen, the lines are vaguely visible); and the lobes are smooth in the descriptive drawing.

Fig. 3.16. (continued on next page). *Tergilatus sparsus* Meyer & Ueckermann, 1995, leaf vagrant on *Portulacaria afra*: SEM images (a, d, f, h, j), line drawings (c, d, g) [from Meyer & Ueckermann (1995)],and slide mounted specimens viewed with phase contrast (b, i, j, k): **a)** dorsal view; **b, c)** lateral view; **d)** ventral view; **e, f)** enlargement of opisthosomal microtubercles, alternatively lateral and dorsal; **g, h)** dorsal view; **i)** dorsal view of opisthosomal rear end; **j, k, l)** prodorsum (lateral in j, dorsal in k, l) including rear shield margin and first dorsal annuli; **a, d, h, l)** scale lines = 10 µm; **f)** scale line = 1 µm. Open arrows - rear end of opisthosoma; solid black arrows - first annulus behind rear prodorsal shield margin, orange arrow - pointing towards dorsal microtubercles in drawing and SEM image.

Fig. 3.17. *Tetra retusa* Meyer, 1992 from *Bauhinia galpinii* (Meyer, 1992b): **a, c, e)** wax secretions and enlargements thereof on about the entire body, but particularly on the ridges of the opisthosoma and prodorsal shield, all specimens in dorsal view; **b)** descriptive drawing (Meyer, 1992b) in dorsal view, without the wax, which was also not mentioned in the text description. *Calacarus* sp. from *Searsia lancea* (previously *Rhus lancea*): **d)** dorso-lateral aspect of the prodorsum with wax formations, the image of a specimen with some of the wax disturbed and broken off was chosen to be presented, to illustrate the inside and structure of wax cells; **a, d, e)** scale lines = 10 µm; **c)** scale line = 1 µm.

Fig. 3.18. Spermatophores of *Aculus* sp. from *Lantana trifolia*: **a)** with sperm packet in tact; **b)** without sperm packet. Possibly *Rhynacus* sp. from *Mystroxylon aethiopicum* subsp. *aethiopicum*: c) eggs and immatures.

Fig. 3.19. Eriophyoid gnathosoma: **a)** dorsal view; **b)** line drawing of gnathosoma in image 3.19a; **c)** ventral view; **d)** line drawing of the gnathosoma in image 3.19c. Scale lines = 1 µm.

Fig. 3.20. (continued on next page). Gnathosoma of a *Calacarus* sp. (Eriophyidae: Phyllocoptinae: Calacarini): **a)** ventral view; **b)** ventro-lateral view; **c)** line drawing of image 3.20a; **d)** line drawing of image 3.20b; **a)** scale line = 1 µm; **b, c, d)** scale lines = 10 µm. * These are preliminary new names or terms devised in the present study for these gnathosomal structures on the ventral aspect of eriophyoid mites. ** This structure was named the "basal palp segment" (Keifer, 1975a) or the "oral plate". It is just ahead of the coxal plates of coxae I, and it is situated about on the same vertical level as the pharyngeal pump.

Fig. 3.20. (continued from previous page). Eriophyoid gnathosomas in ventral view. *Trisetacus* sp. *cf. T. pinastri* Nuzzaci, 1975 (Phytoptidae: Nalepellinae: Trisetacini) from a *Pinus* sp.: **e)** SEM image; **f)** line drawing of image 3.20e. *Shevtchenkella* sp. *cf. S. lividae* (Meyer, 1990) (Eriophyidae: Phyllocoptinae: Tegonotini) from *Psydrax livida*: **g)** SEM image; **h**) line drawing of image 3.20g; **e, f)** scale lines = 10 µm; **g, h)** scale lines = 1 µm. Key to colours in drawings on previous page.

Fig. 3.21. Eriophyoid gnathosoma: Ventral views of the mostly the infracapitulum and part of the pedipalpi and palpcoxal plate of various species to show the differences in structures. The shape of the ventral part of the stylet sheath is visible between the free palp-segments. Its shape is probably strongly influenced by the angle at which imaged, and the anteriad extension of the gnathosoma at the moment of cryo freezing. However, there are some obvious differences in shape not influenced by these factors, that may be of use in classification and phylogeny. The data was not evaluated and this figure purely demonstrates that there are indeed differences that may be of systematic use. The colours correspond to probably homologous areas between the species, and the key to the colours is given on the first page of Fig. 3.20. The longer scale lines = 10 µm, and the three shortest scale lines = 1 µm.

Fig. 3.22. Eriophyoid gnathosoma. The gnathosoma of all the Eriophyoidea except the Diptilomiopidae has relatively short and straight chelicerae, and the short-form oral stylet: **a)** digital image of slide-mounted specimen viewed with light microscope; **c)** SEM image of lateral view. "Diptilomiopid"-like gnathosoma with large chelicerae sharply bent down at the base and the long-form oral stylet: **b)** digital image of slide-mounted specimen, **d, e)** lateral views of gnathosomas. Scale lines = 10 µm.

Fig. 3.23. Different hypotheses regarding the homology of the pedipalpal segments of the Eriophyoidea with other Acariform pedipalpi: **a, b)** segments according to Lindquist (1996a), *but according to him the first free segment is a fusion of the trochanter, femur and genu, the genu, however, is dorsally fused with the other segments, but ventrally separated from them; **c)** segments according to Keifer (1959a); **d)** segments according to Keifer (1975a).
Scale lines = 10 µm.

Fig. 3.24. Dorsal view of gnathosomas of **a)** *Cecidophyopsis selachodon*; **b)** *C. grossulariae*; **c)** *C. aurea* and **d)** *C. alpina*. cr = cheliceral retainer. Below drawings with species names are the descriptions of the cheliceral retainers from Amrine *et al.* (1994). Cheliceral retainers of *C. ribis* are not depicted in Amrine *et al.* (1994). Drawings were scanned from Amrine *et al.* (1994) (with permission from the author), and were cropped and enlarged or made smaller so that scale lines (10 µm) are all the same length, and thus drawings are at about the same scale.

Fig. 3.25. Gnathosoma of *Trisetacus* sp. *cf. T. pinastri* Nuzzaci, 1975 (Phytoptidae: Nalepellinae: Trisetacini) from *Pinus pinaster*: **a, b)** dorsal views (probably adults, gender unknown), blue arrows are indicating droplet-like structures that are probably not part of the mite, but artefacts; **c)** line drawing of image 3.25a, red line indicating length of palpcoxal base, blue line indicating distance of seta *ep* from distal margin of palpcoxal base, from base of seta, shortest distance to apical margin; **d)** line drawing of enlargement of "cheliceral lock mechanism" in dorsal view image 3.25b; **e)** dorsolateral view (probably adult, gender unknown); **f)** ventral view (male). Scale lines = 10µm.

Fig. 3.26. Gnathosoma of *Setoptus radiatae* Meyer, 1991 (Phytoptidae: Nalepellinae: Nalepellini) from *Pinus radiata*: **a)** dorsal view (probably adult, gender unknown); **b)** ventral view (female); **c)** line drawing of image 3.26a; **d)** lateral view (probably adult, gender unknown). Scale lines = 10µm.

Fig. 3.27. Gnathosoma of *Mackiella* sp. (Phytoptidae: Sierraphytoptinae: Mackiellini) from *Phoenix reclinata*: **a)** dorsal view (probably adult, gender unknown); **b)** line drawing of image 3.27a; **c)** lateral view (male); **d)** ventral view (male); **e)** line drawing of image 3.27d; **a, b)** scale lines = 1 µm; **c, d, e)** scale lines = 10 µm.

Fig. 3.28. Gnathosoma of *Aberoptus* sp. *cf. Aberoptus* sp. nov. (Eriophyidae: Aberoptinae) from *Schotia brachypetala*: **a)** dorsal view (probably adult, gender unknown); **b)** lateral view (female); **c)** line drawing of image 3.28a, red line indicating length of palpcoxal base, blue line indicating distance of seta *ep* from distal margin of palpcoxal base, from base of seta, shortest distance to apical margin; **d)** ventral view (female); **a, c)** scale lines = 1 µm; **b, d)** scale lines = 10 µm.

Fig. 3.29. (continued on next page). Gnathosoma of *Cecidophyopsis* sp. *cf. Cecidophyopsis hendersoni* (Keifer, 1954) (Eriophyidae: Cecidophyinae: Cecidophyini) from *Yucca guatemalensis*: **a)** dorso-lateral view (female); **b)** dorsal view (possibly immature based on gnathosoma morphology); **c)** line drawing of image 3.29a, showing broken off setae which is possibly an artefact caused by cryo-praparation; **d)** enlargement of protuberances basally on the chelicerae; **e)** dorso-lateral view of gnathosoma of just-born larva still emerging from egg; **a, c, e)** scale lines = 10 µm; **d)** scale line = 1 µm.

Fig. 3.29. (continued from previous page). Gnathosoma of *Cecidophyopsis* sp. *cf. Cecidophyopsis hendersoni*: **f)** ventral view (female); **g)** lateral view, gnathosoma with apical palp segments telescoping for feeding (female); **h)** lateral view (female); **i)** line drawing of image 3.29j; **j)** ventro-lateral view of gnathosoma (female); **f, g, h, j)** scale lines = 10 µm; **i)** scale line = 1 µm.

Fig. 3.30. Gnathosoma of *Afromerus lindquisti* Meyer, 1990 (Eriophyidae: Cecidophyinae: Colomerini) from *Psydrax livida*: **a)** dorsal view (female); **b, c)** ventro-lateral views (males); **a, b)** scale lines = 1 µm; **c)** scale line = 10 µm.

Fig. 3.31. Gnathosoma of *Ectomerus* sp. *cf. E. systenus* Meyer, 1990 (Eriophyidae: Cecidophyinae: Colomerini) from *Terminalia sericea*: **a)** dorsal view (probably adult, gender unknown); **b)** ventral view (female); **c)** dorso-lateral view (probably adult, gender unknown); **a, c)** scale lines = 1 µm; **b)** scale line = 10 µm.

Fig. 3.32. Gnathosoma of *Neserella* sp. *cf. N. tremae* Meyer & Ueckermann, 1989 (Eriophyidae: Cecidophyinae: Colomerini) from *Trema orientalis*: **a)** dorsal view (probably adult, gender unknown); **b)** dorso-lateral view (immature); **c)** lateral view (probably adult, gender unknown); **d)** line drawing of image 3.32b; **e)** ventral view (female); **a, b, d)** scale lines = 1 µm; **c, e)** scale lines = 10 µm.

Fig. 3.33. (continued on next page). Gnathosoma of *Acalitus mallyi* (Tucker, 1926) (Eriophyidae: Eriophyinae: Aceriini) from *Vangueria infausta* subsp. *infausta* leaf galls: **a)** dorsal view (probably adult, gender unknown); **b)** digitally captured image of dorsal view of a slide-mounted female specimen; **c)** line drawing of image 3.33a; **d)** line drawing of part of image 3.33b; **a, c)** scale lines = 1 µm; **b, d)** scale lines = 20 µm.

Fig. 3.33. (continued from previous page). Gnathosoma of *Acalitus mallyi*: **e)** ventral view (female); **f)** ventro-lateral view (female); **g)** lateral view (female); **h)** line drawing of image 3.33f; **i)** line drawing of image 3.33g; **j)** digital image captured of slide-mounted female specimen, outline of flap extension of coxal plate very unclear, traced with a red stipple line; a knob-like structure in a hollow formed by the anterior edge of the ventral coxal base indicated by the green arrows; **e, g, i)** scale lines = 10 µm; **f, h)** scale lines = 1 µm; **j)** scale line = 20 µm.

Fig. 3.34 (continued on next page). Gnathosoma of *Aceria lantanae* (Cook, 1909) (Eriophyidae: Eriophyinae: Aceriini) from *Lantana* x *camara* (hybrid complex) flower galls: **a, b)** dorsal views (probably adults, gender unknown); **c)** line drawing of image 3.34a; **d)** enlargement of cheliceral protuberances in image 3.34b. Scale lines = 1 µm.

Fig. 3.34. (continued from previous page). Gnathosoma of *Aceria lantanae*: **e)** lateral view (female); **f)** line drawing of image 3.34e; **g, h)** ventral views of the same specimen (female); **e, f, g)** scale lines = 1 µm; **h)** scale line = 10 µm.

Fig. 3.35. Gnathosoma of *Aceria ocellatum* Meyer & Ueckermann, 1990 (Eriophyidae: Eriophyinae: Aceriini) from *Searsia lancea* (previously *Rhus lancea*) leaf galls: **a)** dorsal view (probably adult, gender unknown); **b)** dorsal view (immature); **c)** dorso-lateral view (probably adult, gender unknown); **a)** scale line = 1 µm; **b, c)** scale lines = 10 µm.

Fig. 3.36. Gnathosoma of *Aceria* sp. *cf. A. dichrostachyia* (Tucker, 1926) (Eriophyidae: Eriophyinae: Aceriini) from *Dichrostachys cinerea* subsp. and var. unknown: **a)** dorso-lateral view (probably adult, gender unknown); **b)** dorso-lateral view (larva); **c)** line drawing of image 3.36a; **d, e)** lateral view of the same specimen (female); **f)** ventral view (female); **a, c)** scale lines = 10 µm; **b, d, e, f)** scale lines = 1 µm.

Fig. 3.37. Gnathosoma of *Aceria* sp. *cf. A. giraffae* Meyer, 1990 (Eriophyidae: Eriophyinae: Aceriini) from *Acacia erioloba*: **a)** dorsal view (probably adult, gender unknown); **b)** ventro-lateral view (female); **c)** enlargement of cheliceral protuberances in image 3.37a; **d)** dorso-lateral view (probably adult, gender unknown); **a, b)** scale lines = 10 µm; **d)** scale line = 1 µm.

Fig. 3.38. Gnathosoma of *Aceria* sp. nov. (Eriophyidae: Eriophyinae: Aceriini) from *Chrysanthemoides incana*: **a)** dorsal view (probably adult, gender unknown); **b)** line drawing of image 3.38a; **c)** lateral view (female); **d)** ventral view (female); **e)** ventral view (male); **a, b, c, e)** scale lines = 1 µm; **d)** scale line = 10 µm.

Fig. 3.39. Gnathosoma of *Aceria* sp. nov. females (Eriophyidae: Eriophyinae: Aceriini) from *Chrysanthemoides monilifera* subsp. *monilifera*: **a)** dorso-lateral view; **b)** ventro-lateral view; **c)** lateral view; **d)** ventro-lateral view of apical tip of the pedipalpi; **a, b)** scale lines = 10 µm; **c, d)** scale lines = 1 µm.

Fig. 3.40. Gnathosoma of *Aceria* sp. *cf. A. proteae* Meyer, 1981 (Eriophyidae: Eriophyinae: Aceriini) from *Protea caffra* subsp. *caffra*: **a)** dorsal view (probably adult, gender unknown); **b)** dorsal view (larva); **c)** lateral view (female); **d, e)** ventro-lateral views (females); **a, b, e)** scale lines = 1 µm; **c, d)** scale lines = 10 µm.

Fig. 3.41. (continued on next page). Gnathosoma of *Aceria* sp. *cf. Aceria* sp. nov. (Eriophyidae: Eriophyinae: Aceriini) from *Ipomoea batatas* var. *batatas*: **a)** dorso-lateral view (probably adult, gender unknown); **b)** dorsal view (probably larva); **c)** enlargement of cheliceral protuberances in 3.41a; **d)** line drawing of image 3.41a. Scale lines = 1 µm.

Fig. 3.41. (continued from previous page). Gnathosoma of *Aceria* sp. *cf. Aceria* sp. nov.: **e)** dorso-lateral view (male); **f)** lateral view of basal part of gnathosoma (female); **g)** ventro-lateral view (female); **h)** ventral view (female); **e, h)** scale lines = 10 µm; **f, g)** scale lines = 1 µm.

Fig. 3.42. (continued on next page). Gnathosoma of *Aceria* sp. *cf. Aceria* sp. nov. (Eriophyidae: Eriophyinae: Aceriini) from *Oxalis corniculata*: **a)** dorsal view (probably adult, gender unknown), white arrows indicate seta *ep* (closest to chelicerae), and two protuberances on the side of it; **b)** line drawing of image 3.42a; **c)** enlargement of cheliceral protuberances in image 3.42a; **d)** enlargement of seta ep on the right hand side of the specimen in 3.42a and the first protuberance alongside it; **e)** enlargement of seta *ep* and two protuberances indicated by white arrows in image 3.42a, also here indicated by white arrows; **f)** seta *ep*, and seta (still unnamed, but mentioned in the text description) alongside it on the gnathosomal palpcoxal base of *Acaphyllisa limitata* (redrawn from Flechtmann & Etienne, 2001), which might be homologous with the first protuberance alongside seta *ep* in the *Aceria* sp. from *O. corniculata*; **g)** lateral view (probably adult, gender unknown) with black arrows indicating the first protuberance next to seta *ep*. Scale lines = 1 µm.

Fig. 3.42. (continued from previous page).Gnathosoma of *Aceria* sp. *cf. Aceria* sp. nov.: **h)** ventro-lateral view (male), some detail enhanced with black drawing line to make it more visible; **i)** ventro-lateral view (male); **h)** scale line = 10 µm; **i)** scale line = 1 µm.

Fig. 3.43. Gnathosoma of *Aceria* sp. *cf. Aceria* sp. nov. (Eriophyidae: Eriophyinae: Aceriini) from *Acacia rehmanniana*: **a)** dorso-lateral view (probably adult, gender unknown); **b)** dorso-lateral view (larva), some lines traced in black to make them more clear; **c)** enlargement of cheliceral protuberances in image 3.43a; **d)** ventral view (female); **e)** ventro-lateral view (female); **f)** lateral view (female); a rounded bump each side laterally on ventral palpcoxal base (indicated by white arrows in images e and f; **a, b, f)** scale lines = 1 µm; **d, e)** scale lines = 10 µm.

Fig. 3.44. (continued on next page). Gnathosoma of unknown genus, nr. *Aceria* (Eriophyidae: Eriophyinae: Aceriini) from *Apodytes dimidiata* subsp. *dimidiata* flower buds: a, **b)** dorsal views (the same specimen, probably adult, gender unknown); **c)** line drawing of image 3.44a; **d)** enlargement of cheliceral protuberances in 3.44b. Scale lines = 1 µm.

Fig. 3.44. (continued from previous page). Gnathosoma of unknown genus, nr. *Aceria*: **e)** ventro-lateral view (male); **f)** dorso-lateral view (probably adult, gender unknown); **g)** line drawing of image 3.44e; **h)** ventro-lateral view (female); **e, g, h)** scale lines = 1 µm; **b)** scale line = 10 µm.

Fig. 3.45. Gnathosoma of *cf. Aceria* sp. (Eriophyidae: Eriophyinae: Aceriini) from *Cineraria* sp. blisters: **a)** lateral view (female); **b, d)** ventral views of the same specimen (female); **c)** dorsal view (probably adult, gender unknown); **a, c)** scale lines = 1 µm; **b, d)** scale lines = 10 µm.

Fig. 3.46. Gnathosoma of *Aceria* sp. (probably a new species) (Eriophyidae: Eriophyinae: Aceriini) from *Xymalos monospora*: **a)** dorsal view (probably adult, gender unknown); **b, c)** ventral views of the same specimen (female); lateral view (female); **a, c)** scale lines = 10 µm; **b, d)** scale lines = 1 µm.

Fig. 3.47. Gnathosoma of *Tumescoptes* sp. *cf. T. dicrus* (Eriophyidae: Phyllocoptinae: Acaricalini) from *Phoenix reclinata*: **a)** ventro-dorsal view (female); **b)** bifurcate setae *d* enlarged to show tiny side branch (probably adult, gender unknown); **c)** enlargement of cheliceral protuberance in image 3.47a; **d)** venro-lateral view (female). Scale lines = 1 µm.

Fig. 3.48. (continued on next page). Gnathosoma of a *Calacarus* sp. (Eriophyidae: Phyllocoptinae: Calacarini) from *Searsia lancea* (previously *Rhus lancea*): **a)** lateral view (female); **b)** dorso-lateral view (female); **c)** line drawing of image 3.48a. Scale lines = 10 µm.

Fig. 3.48. (continued from previous page). Gnathosoma of a *Calacarus* sp.: **d)** ventral view (female); **e)** ventro-lateral view (female); **f)** line drawing of "oral plate" area of image 3.48d, names for different areas are preliminary. Scale lines = 10 µm.

Fig. 3.49. Gnathosoma of a *Calacarus* sp. (Eriophyidae: Phyllocoptinae: Calacarini) from *Faurea rochetiana*: **a, b)** lateral view of the same specimen (probably adult, gender unknown). Scale lines = 10 µm.

Fig. 3.50. Gnathosoma of a *Calacarus* sp. (Eriophyidae: Phyllocoptinae: Calacarini) from *Psydrax livida*: **a)** dorsal view (probably adult, gender unknown), in vagrants, like this *Calacarus* sp., the frontal lobe obscures the gnathosoma which is also usually more hypognathous in these species, in dorsal view; **b)** lateral view (probably adult, gender unknown); **c, d)** ventro-lateral views of the same specimen (female); **a, b, c)** scale lines = 10 µm; **d)** scale line = 1 µm.

Fig. 3.51. Gnathosoma of a *Shevtchenkella* sp. *cf. S. lividae* (Meyer, 1990) (Eriophyidae: Phyllocoptinae: Tegonotini) from *Psydrax livida*: **a)** gnathosoma obscured by frontal lobe in dorsal view (probably adult, gender unknown); **b)** dorso-lateral view (male); **c)** ventral-dorsal view (female), note extrusion of possibly several gnathosomal stylets closely fitted against each other from the stylet sheath; **d)** ventro-lateral view male; **a, b, d)** scale lines = 10 µm; **c, e)** scale lines = 1 µm.

Fig. 3.52. Gnathosoma of a *Shevtchenkella* sp. *cf. S. rhusi* (Meyer, 1990) (Eriophyidae: Phyllocoptinae: Tegonotini) from *Searsia lancea* (previously *Rhus lancea*): **a)** frontal lobe largely obscures gnathosoma in dorsal view (probably adult, gender unknown); **b)** dorso-lateral view (probably adult, gender unknown); **c)** ventro-lateral view (female); **a, c)** scale lines = 10 µm; **b)** scale line = 1 µm.

Fig. 3.53. Gnathosoma of a *Neoshevtchenkella* or *Shevtchenkella* sp. (with wax) (Eriophyidae: Phyllocoptinae: Tegonotini) from *Celtis africana*: **a)** dorso-ventral view (female); **b)** lateral view (female). Scale lines = 10 µm.

Fig. 3.54. Gnathosoma of a genus *cf. Calepitrimerus* (Eriophyidae: Phyllocoptinae: Phyllocoptini) from *Celtis africana*: **a, b)** ventral view of the same specimen (female); **c)** dorso-lateral view (female); **d)** enlargement of cheliceral protuberances in image 3.54c; **e)** dorso-lateral view (probably adult, gender unknown); **a, e)** scale lines = 1 µm; **b, c)** scale lines = 10 µm.

Fig. 3.55. Gnathosoma of *Cecidodectes euzonus* Nalepa, 1917 (Eriophyidae: Phyllocoptinae: Phyllocoptini) from *Trema orientalis*: **a)** dorso-lateral view (probably adult, gender unknown); **b)** ventro-lateral view (female); **c)** lateral view (probably adult, gender unknown); **d)** ventro-lateral view (female); **a)** scale line = 1 µm; **b, c, d)** scale lines = 10 µm.

Fig. 3.56. Gnathosoma of a *cf. Phyllocoptes* sp. (Eriophyidae: Phyllocoptinae: Phyllocoptini) from *Anthocleista grandiflora*: **a)** dorsal view (probably adult, gender unknown); **b)** enlargement of the cheliceral protuberances in 3.56a; **c)** lateral view (female); **d)** line drawing of cheliceral protuberances in 3.56a and enlarged in 3.56b; **e, f)** ventral views (females); **a, c, f)** scale lines = 1 µm; **e)** scale line = 10 µm.

Fig. 3.57. (continued on next page). Gnathosoma of *Tergilatus sparsus* Meyer & Ueckermann, 1995 (Eriophyidae: Phyllocoptinae: Phyllocoptini) from *Portulacaria afra*: **a)** dorsal view (female); **b)** dorso-lateral view (larva); **c)** enlargement of cheliceral protuberances in image 3.57a; **d)** line drawing of image 3.57b; **a)** scale line = 10 µm; **b, d)** scale lines = 1 µm.

Fig. 3.57. (continued from previous page). Gnathosoma of *Tergilatus sparsus*: **e)** ventro-lateral view (male); **f)** ventral view (immature, stage unknown); **g)** ventro-lateral view (female). Scale lines = 10 µm.

Fig. 3.58. Gnathosoma of possibly an *Aculops* or *Metaculus* sp. (Eriophyidae: Phyllocoptinae: Anthocoptini) from *Anthocleista grandiflora*: dorso-lateral view (probably adult, gender unknown). Scale line = 10 µm.

Fig. 3.59. Gnathosoma of an *Aculus* sp. *cf. Aculops lycopersici* (Eriophyidae: Phyllocoptinae: Anthocoptini) from *Physalis peruviana*: **a)** dorso-ventral view (female); **b)** enlargement of cheliceral protuberances in image 3.59a; **c)** lateral view (female); **d)** dorso-lateral view (female); ventral view (female); **a, d, e)** scale lines = 10 µm; **c)** scale line = 1 µm.

Fig. 3.60. Gnathosoma of a *cf. Aculus* sp. (Eriophyidae: Phyllocoptinae: Anthocoptini) from *Acacia burkei*: **a, c, d)** lateral views of different areas and enlargements of the same female specimen; **b)** line drawing of the cheliceral protuberances in image 3.60a (also enlarged in 3.60d); **e)** dorso-lateral view, basal part of gnathosoma obscured by frontal lobe (probably adult, gender unknown). Scale lines = 1 µm.

Fig. 3.61. Gnathosoma of a *cf. Aculus* sp. (Eriophyidae: Phyllocoptinae: Anthocoptini) from *Lantana trifolia*: **a)** dorso-lateral view (probably adult, gender unknown); **b)** dorsal view (probably adult, gender unknown); **c)** basal part, dorso-lateral view (probably adult, gender unknown); **d)** enlargement of cheliceral protuberances in image 3.61b; **e)** distal part, ventro-lateral view (female); **f)** oral plate region, ventro-lateral view (female, same specimen as 3.61e); **g)** distal part, lateral view (female); **h)** basal part, lateral view (female); **a, b, c, e, h)** scale lines = 1 µm; **f, g)** scale lines = 10 µm.

Fig. 3.62. Gnathosoma of a *cf. Aculus* sp. or possibly an immature of *Quantalitus* (Eriophyidae) from *Rothmannia capensis*: **a)** dorsal view, frontal lobe obscures most of gnathosoma (possibly immature); **b)** lateral view (immature). Scale lines = 10 µm.

Fig. 3.63. Gnathosoma of *Costarectus zeyheri* Meyer & Ueckermann, 1995 (Eriophyidae: Phyllocoptinae: Anthocoptini) from *Dovyalis zeyheri*: **a)** dorso-lateral view (adult, probably female); **b)** dorso-lateral view (male); **c)** lateral view (female); **d)** ventro-lateral view (female); **a, b, d)** scale lines = 10 µm; **c)** scale line = 1 µm.

Fig. 3.64. Gnathosoma of *Meyerella bicristatus* (Meyer, 1989) females (Eriophyidae: Phyllocoptinae: Anthocoptini) from *Mystroxylon aethiopicum*: **a, c, f)** ventro-dorsal view of the same specimen, are with cheliceral protuberances in image 3.64a enlarged in c and further enlarged in f; **b)** ventral view; **d)** lateral view; **e)** ventrolateral view; **g)** line drawing of image 3.64e; **a, b, c, e)** scale lines = 1 µm; **d)** scale line = 10 µm.

Fig. 3.65. (continued on next page). Gnathosoma of possibly a new genus (according to traditional taxonomic criteria) nr. *Costarectus* (Eriophyidae: Phyllocoptinae: Anthocoptini) from *Mystroxylon aethiopicum*: **a)** dorso-lateral view (probably adult, gender unknown); **b, e)** lateral views of the same specimen (male); **c)** enlargement of cheliceral protuberances in image 3.65a; **d)** dorsal view to show the shape of the dorsal pedipalp genual setae (setae *d*) (probably adult, gender unknown); **a, d, e)** scale lines = 1 µm; **b)** scale line = 10 µm.

Fig. 3.65. (continued from previous page). Gnathosoma of possibly a new genus (according to traditional taxonomic criteria) nr. *Costarectus*: **f)** ventro-lateral view (male); **g)** ventral view (male); **h)** line drawing of image 3.65g. Scale lines = 10 µm.

Fig. 3.66. Gnathosoma of possibly a new genus (according to traditional taxonomic criteria) nr. *Tetra* (Eriophyidae: Phyllocoptinae: Anthocoptini) from *Protea caffra* subsp. *caffra*: **a)** dorso-lateral view (probably adult, gender unknown); **b)** ventro-lateral view (female). Scale lines = 10 µm.

Fig. 3.67. Gnathosoma of possibly a new genus (according to traditional taxonomic criteria) nr. *Mesalox* (Eriophyidae: Phyllocoptinae: Anthocoptini) from *Apodytes dimidiata*: **a)** dorsal view (probably adult, gender uknown); **b)** lateral view (female); **c)** ventro-dorsal view (female); **d)** ventro-lateral view (female); **e)** enlargement of the cheliceral protuberances in image 3.67a; **f)** ventral view (male); **a, c)** scale lines = 1 µm; **b, d, f)** scale line = 10 µm.

Fig. 3.68. Gnathosoma of *Porosus monosporae* Meyer & Ueckermann, 1995 (Eriophyidae: Phyllocoptinae: Anthocoptini) from *Xymalos monosporae*: **a)** ventro-lateral view (female); **b)** ventral view (female); **c)** ventro-lateral view (male); **a, b)** scale lines = 10 µm; **c)** scale line = 1 µm.

Fig. 3.69. Gnathosoma of a *Tegolophus* sp. *cf. T. orientalis* Meyer, 1990 (Eriophyidae: Phyllocoptinae: Anthocoptini) from *Trema orientalis*: **a)** ventro-lateral view (female); **b)** lateral view (female). Scale lines = 10 µm.

Fig. 3.70. (continued on next page). Gnathosoma of *Tetra retusa* Meyer, 1992 (Eriophyidae: Phyllocoptinae: Anthocoptini) from *Bauhinia galpinii*: **a)** dorso-lateral view (probably adult, gender unknown); **b)** enlargement of cheliceral protuberances in image 3.70a; **c)** dorsal view (probably adult, gender unknown). Scale lines = 10 µm.

Fig. 3.70. (continued from previous page). Gnathosoma of *Tetra retusa*: **d)** ventro-lateral view (female); **e)** lateral view (female); **f)** dorso-lateral view (larva); **g)** ventral view (female); **h)** ventral view (male); **d, e, f)** scale lines = 1 µm; **g, h)** scale lines = 10 µm.

Fig. 3.71. Gnathosoma of a *Tetraspinus* sp. (Eriophyidae: Phyllocoptinae: Anthocoptini) from *Chrysanthemoides monilifera monilifera*: **a)** dorso-ventral view (female); **b)** enlargement of cheliceral protuberances in image 3.71a; **c, d)** lateral views (females); **e)** dorso-lateral view (probably adult, gender unknown); **a, c, d)** scale lines = 10 µm; **e)** scale lines = 1 µm.

Fig. 3.72. Gnathosoma of a *cf. Tetraspinus* sp. (Eriophyidae: Phyllocoptinae: Anthocoptini) from *Faurea rochetiana*: **a)** dorso-lateral view (probably adult, gender unknown); **b)** lateral view (female); **c)** dorso-ventral view (female); **d)** lateral view (female); **e)** enlargement of cheliceral protuberances; **a)** scale line = 1 µm; **b, c, d)** scale lines = 10 µm.

Fig. 3.73. (continued on next page). Gnathosoma of a possibly new worm-like genus (according to traditional taxonomic criteria) (Eriophyidae: Eriophyinae?: Aceriini?) from *Faurea rochetiana*: **a)** dorsal view (probably adult, gender unknown); **b)** dorso-lateral view (probably adult, gender unknown); **c)** dorso-lateral view (probably adult, gender unknown); **d)** line drawing of image 3.73a. Scale lines = 1 µm.

Fig. 3.74. Gnathosoma of an unknown genus (could not be identified) (Eriophyidae: Phyllocoptinae?) from *Ekebergia capensis*: ventral view (male). Scale line = 10 µm.

Fig. 3.75. Gnathosoma of a possibly new genus (according to traditional taxonomic criteria) in the Phyllocoptinae or Cecidophyinae (Eriophyidae) from *Acacia burkei*: **a)** lateral view (possibly nymph); **b)** same specimen as 3.75a, enlargement of cheliceral protuberances; **c, f)** ventral view of the same specimen (female); **d)** dorsal view, gnathosoma obscured by frontal lobe (probably adult, gender unknown); **e)** line drawing of image 3.75g; **g)** lateral view (female) with dorso-ventrally flattened and oval shaped setae *v*; **a, d, f)** scale lines = 10 µm; **b, c, g)** scale lines = 1 µm.

Fig. 3.76. Gnathosoma of a *Phyllocoptes* sp. (Phyllocoptinae) or new genus (Cecidophyinae) from *Dovyalis zeyheri*: **a)** dorsal view, basal part of gnathosoma obscured by frontal lobe (probably adult, gender unknown); **b)** ventral view (male); **c)** lateral view of basal part of gnathosoma (female); **d)** ventro-lateral view (female); **e)** lateral view of distal part of gnathosoma (female); **f)** dorso-lateral view (larva); **a, d)** scale lines = 1 µm; **b, c, e, f)** scale lines = 10 µm.

Fig. 3.77. Gnathosoma of a probably new genus (according to traditional taxonomic criteria) (Eriophyidae, subfamily uncertain) from *Cussonia* sp. flowers: **a)** dorso-lateral view (probably adult, gender unknown); **b, d)** ventro-lateral views of the same specimen (female); **c)** enlargement of cheliceral protuberances in image 3.77a; **e)** lateral view (female); **f)** ventral view (male); **a, d, e, f)** scale lines = 10 µm; **b)** scale line = 1 µm.

Fig. 3.78. Gnathosoma of *Diptilomiopus apobrevus* sp. nov. (Diptilomiopidae: Diptilomiopinae) from *Apodytes dimidiata*: **a)** dorso-lateral view (probably adult, gender unknown); **b)** ventro-dorsal view (female); **c)** dorso-lateral view (larva); **d)** ventro-lateral view (female); **e)** lateral view, basal part (possibly nymph, or male); **f)** ventro-lateral view, apical part (female); **g)** ventral view (female). Scale lines = 10 µm.

Fig. 3.79. Gnathosoma of *Diptilomiopus faurius* sp. nov. (Diptilomiopidae: Diptilomiopinae) from *Faurea rochetiana*: **a)** dorsal view (probably adult, gender unknown); **b)** lateral view (female); **c)** dorso-lateral view, basal part (female); **d, e)** ventro-lateral views of the same specimen (female); lateral view (distal part of gnathosoma); **a, b, d)** scale lines = 10 µm; **c, e, f)** scale lines = 1 µm.

Fig. 3.80. Gnathosoma of an unknown species (species could not be identified) (Diptilomiopidae: Diptilomiopinae) from *Xymalos monospora*: **a)** dorso-lateral view (probably adult, gender unknown); **b)** ventro-lateral view (female); **c)** ventral view (male); **d)** lateral view (female); **a, b, d)** scale lines = 10 µm; **c)** scale line = 1 µm.

Fig. 3.81. Gnathosoma of probably a new genus (according to traditional taxonomic criteria), nr. *Dacundiopus* (Diptilomiopidae: Diptilomiopinae), from *Mystroxylon aethiopicum*: **a)** dorsal view (probably adult, gender unknown); **b)** ventro-dorsal view (female); **c)** dorsal view (immature); **d, e)** lateral views (females); **f)** ventral view (female); ventro-lateral view (female); **a, b, d, e, f, g)** scale lines = 10 µm; **c)** scale line = 1 µm.

Fig. 3.82. Gnathosoma of a probably new *Rhynacus* sp. (Diptilomiopidae: Diptilomiopinae) from *Dovyalis zeyheri*: **a, b)** dorso-lateral view and enlargement of the basal area respectively of the same specimen (probably adult, gender unknown); **c, e)** lateral view and enlargement of the distal part respectively of the same specimen (male); **d)** dorso-lateral view (female); **f)** ventro-lateral view (male); **a, c, d, f)** scale lines = 10 µm; **b, e)** scale lines = 1 µm.

Fig. 3.83. Gnathosoma of probably a new genus (according to traditional taxonomic criteria) (Eriophyidae) from *Searsia lancea* (previously *Rhus lancea*) leaf blisters: **a)** dorsal view (probably adult, gender unknown); **b)** ventral view (immature); **c)** preliminary attempt at a line drawing (which is probably still wrong and incomplete, because the SEM images that could be obtained from this species were extremely unclear, probably due to a sticky substance covering the mites) of the dorsal view of the gnathosoma, from image 3.83a; **d)** lateral view (probably adult, gender unknown); **a, c, d)** scale lines = 1 µm; **b)** scale line = 10 µm.

Fig. 3.84. Gnathosoma of unidentified morphospecies two (Eriophyoidae: Eriophyidae or Phytoptidae, but it is probably Eriophyidae) from green fruit of *Anthocleista grandiflora*: **a)** dorso-lateral view (probably adult, gender unknown); **b)** dorsal view (larva); **c, f)** lateral views of the same specimen (probably adult, gender unknown); **d)** ventral view (female); **e)** ventral view (male); **a, b, c)** scale lines = 1 µm; **d, e, f)** scale lines = 10 µm.

Fig. 3.85. Gnathosoma of an unknown species (could not be identified) (Eriophyidae) from *Sideroxylon inerme* subsp. *inerme*: **a)** dorso-lateral view (probably adult, gender unknown); **b)** dorso-lateral view (female); **c)** ventro-lateral view (female); **d)** ventro-lateral view (female); **e)** lateral view (female); **f)** ventro-lateral view (female); **a, b, c)** scale lines = 1 µm; **d, e, f)** scale lines = 10 µm.

Fig. 3.86. Examples of loss of quality of SEM images of species in the current study, in the publishing and photocopying processes, all printed images scanned with the same scanner in Grayscale at a resolution of 200 dpi, and saved as *.tiff: **a)** original printed image Fig. 6, p. 232 in Huang (1992); **b)** photocopy of image received from library, before the original reprint was obtained; **c, d)** photocopies of SEM images (Plate 1 image A and B here c and d alternatively) originally published on p. 441 in Chandrapatya & Boczek (1991b), original article / reprint or original SEM images not yet obtained.

CHAPTER 4

Fig. 4.1. *Orfareptydeus stepheni* Ueckermann & Grout, 2007 (Tydeidae: Tydeinae). Female: **a)** dorsal view; **b)** ventral view; **c)** palp; **d)** leg I; **e)** leg II. Original drawings in Ueckermann & Grout (2007), used with permission.

Fig. 4.2. *Mononychellus yemensis* Meyer, 1996 (Tetranychidae). Female: **a)** dorsal view [setae *h2* not included in original drawing by Meyer (1996)]; **b)** enlargement of lobes on dorsal striae; **c)** ventral view; **d)** apotele of tarsus I. Drawings a, b and d modified from Meyer (1996), drawing c original drawing by author from holotype.

Fig. 4.3. (continued on next page). **a)** Preferred tree of Hong & Zhang (1996a) (redrawn from published tree): strict consensus of 3 equally parsimonious trees found by "branch-and-boud" procedure after the first and second successive reweighting. **b)** Unchanged data of Hong & Zhang (1996a) re-analysed, strict consensus tree (L=80, ci=0.5, ri=0.6) of three shortest trees (each L=77, ci=0.519, ri=0.63) found with implicit enumeration search in TNT under equal weighted characters. Uninformative characters included, white circles homoplasy, black circles characters without any homoplasy, orange circles character state not interrupted (not homoplasious). Unsupported nodes collapsed. Character numbers above, and character states below branches. Tree search in TNT, tree plotted with Winclada. The bars on the right hand sides of the trees indicate families and other taxa. The red bars and text = Phytoptidae, the green bars and text = Eriophyidae and the blue bars and text = Diptilomiopidae. Although the bars indicates subdivisions of families, and largely relationships between them, it doesn't always indicate the order in which the groups occur in the tree, because groups or taxa at one node, or groups in a polytomy do not have "polarity" or "order" and can rotate around the node.

Fig. 4.3 (continued from previous page). **c)** Unchanged data of Hong & Zhang (1996a) re-analysed, preferred tree, implied weighting with k=999, implicit enumeration search resulted in one tree with L=77, ci=51, ri=63. **d)** Same datamatrix, re-analysed with implied weighting, k=3, one tree found. Uninformative characters included, white circles homoplasy, black circles characters without any homoplasy, orange circles character state not interrupted (not homoplasious). Unsupported nodes collapsed. Character numbers above, and character states below branches. Tree search in TNT, tree plotted with Winclada. The bars on the right hand sides of the trees indicate families and other taxa. The red bars and text = Phytoptidae, the green bars and text = Eriophyidae and the blue bars and text = Diptilomiopidae. Although the bars indicates subdivisions of families, and largely relationships between them, it doesn't always indicate the order in which the groups occur in the tree, because groups or taxa at one node, or groups in a polytomy do not have "polarity" or "order" and can rotate around the node.

Fig. 4.4. Estimated consensus tree found with the analysis of the 318 taxon x 117 character data matrix under equal weighting of characters in TNT: entire tree presented to show topology, and it is a metric tree. Total fit = 57.71; Adjusted homoplasy = 72.29; Total length = 5396; CI = 0.056; RI = 0.086. Uninformative characters included. Resolved part of Eriophyoidea clade enlarged in Fig. 4.5. The key to the classification of the terminal species is also applicable to Fig. 4.5.

Fig. 4.5. Estimated consensus tree found with the analysis of the 318 taxon data matrix under equal weighting of characters in TNT (Fig. 4.4): enlarged resolved part of the Eriophyoidea clade. Black numbers above branches are the character numbers of the synapomorphies (encircled in red) or homoplasious characters supporting the nodes, and those in red on terminal branches are autapomorphies. Blue numbers underneath the branches close to the nodes are the node numbers from TNT. Key to colours of and corresponding symbols following species names providing taxonomic classification are given in Fig. 4.4. Blue E-numbers on left are reference numbers for groups found in tree, for inclusion with other trees; informal names of groups discussed in text are on the right.

Fig. 4.6. The strict consensus (Total fit = 72.29; Adjusted homoplasy = 57.71; Total length = 2402; CI = 0.125; RI = 0.623; Nodes = 255) of 32 trees (each - Total fit = 72.36; Adjusted homoplasy = 57.64; Total length = 2347; CI = 0.128; RI = 0.633; Nodes = 316) found with heuristic parsimony analysis of the 318 taxon x 117 character data matrix, using "new technologies" in TNT, with the best score hit 10 times, under implied weighting of characters with k=10. Uninformative characters were included. Unsupported branches were not collapsed. The entire tree is presented to show topology, and it is a metric tree. The bar on the right hand side indicate families and some notes on broad groups and clades. The red bar and text = Phytoptidae, the green bar and text = Eriophyidae and the blue bar and text = Diptilomiopidae. Although the bar indicates subdivisions within families, and largely relationships between them, it doesn't always indicate relationships between the groups correctly, and also not necessarily indicate the order in which the groups occur in the tree, because groups or taxa at one node, or groups in a polytomy do not have "polarity" or "order" and can rotate around the node. The tree is divided into four parts, which are enlarged in Figs 4.7, 4.8, 4.9 and 4.19.

Fig. 4.7. The strict consensus of 32 trees found with heuristic parsimony analysis of the 318 taxon x 117 character data matrix, using "new technologies" in TNT, under implied weighting of characters with k=10 (Fig. 4.6): enlarged part of tree including outgroup species and branch of node with the Eriophyoidea clade. Black numbers above branches are the character numbers of the synapomorphies or homoplasious characters supporting the nodes, and those on the branch supporting node 346 (Eriophyoidea clade) in bold and dark blue are autapomorphies for the Eriophyoidea. The node numbers from TNT are the green numbers underneath the branches and close to the nodes.

Fig. 4.8. The strict consensus of 32 trees found with heuristic parsimony analysis of the 318 taxon x 117 character data matrix, using "new technologies" in TNT, under implied weighting of characters with k=10 (Fig. 4.6): enlarged part of tree including Nalepellinae species group at node numbered one in Fig. 4.6. Black numbers above branches are the character numbers of the synapomorphies (encircled in red) or homoplasious characters supporting the nodes. Green numbers underneath the branches close to the nodes are the node numbers from TNT. Informal names of groups discussed in the text are on the right. Part of tree blocked in grey also occurs, with the same topology, in the estimated consensus tree found from analyzing the 318 taxon data matrix under implied character weighting with k=20 (Fig. 4.26). On the right of terminal taxon names - blue E-numbers are reference numbers for groups found in the estimated consensus tree of the 318 taxon data matrix found under equal character weighting (Fig. 4.5), blue e-numbers are reference numbers for groups found in strict consensus of most parsimonious trees found for 66 taxon data matrix under equal character weighting (Fig. 4.42), red 66 indicates those taxa found in the same groups, or part of same groups, in the strict consensus of most parsimonious trees found for the 66 taxon data matrix under implied character weighting with k=999 (Fig. 4.43). Underlined terminal taxa are included in the 66 taxon data matrix.

Fig. 4.9. The strict consensus of 32 trees found with heuristic parsimony analysis of the 318 taxon x 117 character data matrix, using "new technologies" in TNT, under implied weighting of characters with k=10 (Fig. 4.6): enlarged part of tree at node numbered two in Fig. 4.6, which includes the Eriophyidae and part of the Phytoptidae, to largely show topology. The tree is divided into parts 2A-2I which are enlarged in Figs 4.10-4.18.

Fig. 4.10. The strict consensus of 32 trees found with heuristic parsimony analysis of the 318 taxon x 117 character data matrix, using "new technologies" in TNT, under implied weighting of characters with k=10 (Fig. 4.6) - enlarged part of the group with the Eriophyidae and part of the Phytoptidae (Fig. 4.9): enlarged part 2A. Black numbers above branches are the character numbers of the synapomorphies (encircled in red) or homoplasious characters supporting the nodes. Green numbers underneath the branches close to the nodes are the node numbers from TNT. Parts of tree blocked in grey also occur, with the same topology, in the estimated consensus tree found from analyzing the 318 taxon data matrix under implied character weighting with k=20 (Fig. 4.26). Underlined terminal taxa are included in the 66 taxon data matrix.

Fig. 4.11. The strict consensus of 32 trees found with heuristic parsimony analysis of the 318 taxon x 117 character data matrix, using "new technologies" in TNT, under implied weighting of characters with k=10 (Fig. 4.6) - enlarged part of the group with the Eriophyidae and part of the Phytoptidae (Fig. 4.9): enlarged part 2B. Black numbers above branches are the character numbers of the synapomorphies (encircled in red) or homoplasious characters supporting the nodes. Green numbers underneath the branches close to the nodes are the node numbers from TNT. Informal names of groups discussed in the text are on the right, and indicated with arrows. Parts of tree blocked in grey also occur, with the same topology, in the estimated consensus tree found from analyzing the 318 taxon data matrix under implied character weighting with k=20 (Fig. 4.26). On the right of terminal taxon names - blue e-numbers are reference numbers for groups found in strict consensus of most parsimonious trees found for 66 taxon data matrix under equal character weighting (Fig. 4.42), red 66 indicates those taxa found in the same groups, or part of same groups, in the strict consensus of most parsimonious trees found for the 66 taxon data matrix under implied character weighting with k=999 (Fig. 4.43). Underlined terminal taxa are included in the 66 taxon data matrix.

Fig. 4.12. The strict consensus of 32 trees found with heuristic parsimony analysis of the 318 taxon x 117 character data matrix, using "new technologies" in TNT, under implied weighting of characters with k=10 (Fig. 4.6) - enlarged part of the group with the Eriophyidae and part of the Phytoptidae (Fig. 4.9): enlarged part 2C. Black numbers above branches are the character numbers of the homoplasious characters supporting the nodes. Green numbers underneath the branches close to the nodes are the node numbers from TNT. Parts of tree blocked in grey also occur, with the same topology, in the estimated consensus tree found from analyzing the 318 taxon data matrix under implied character weighting with k=20 (Fig. 4.26). Underlined terminal taxa are included in the 66 taxon data matrix.

Fig. 4.13. The strict consensus of 32 trees found with heuristic parsimony analysis of the 318 taxon x 117 character data matrix, using "new technologies" in TNT, under implied weighting of characters with k=10 (Fig. 4.6) - enlarged part of the group with the Eriophyidae and part of the Phytoptidae (Fig. 4.9): enlarged part 2D. Black numbers above branches are the character numbers of the homoplasious characters supporting the nodes. Green numbers underneath the branches close to the nodes are the node numbers from TNT. Informal name of the group discussed in the text is indicated with an arrow. Part of tree blocked in grey also occurs, with the same topology, in the estimated consensus tree found from analyzing the 318 taxon data matrix under implied character weighting with k=20 (Fig. 4.26). On the right of terminal taxon names - blue E-numbers are reference numbers for groups found in the estimated consensus tree of the 318 taxon data matrix found under equal character weighting (Fig. 4.5), blue e-numbers are reference numbers for groups found in strict consensus of most parsimonious trees found for 66 taxon data matrix under equal character weighting (Fig. 4.42). Underlined terminal taxa are included in the 66 taxon data matrix.

Fig. 4.14. The strict consensus of 32 trees found with heuristic parsimony analysis of the 318 taxon x 117 character data matrix, using "new technologies" in TNT, under implied weighting of characters with k=10 (Fig. 4.6) - enlarged part of the group with the Eriophyidae and part of the Phytoptidae (Fig. 4.9): enlarged part 2E. Black numbers above branches are the character numbers of the homoplasious characters supporting the nodes. Green numbers underneath the branches close to the nodes are the node numbers from TNT. Informal names of the groups discussed in the text are on the right. Part of tree blocked in grey also occurs, with the same topology, in the estimated consensus tree found from analyzing the 318 taxon data matrix under implied character weighting with k=20 (Fig. 4.26). On the right of terminal taxon names - blue E-numbers are reference numbers for groups found in the estimated consensus tree of the 318 taxon data matrix found under equal character weighting (Fig. 4.5). Underlined terminal taxa are included in the 66 taxon data matrix.

Fig. 4.15. The strict consensus of 32 trees found with heuristic parsimony analysis of the 318 taxon x 117 character data matrix, using "new technologies" in TNT, under implied weighting of characters with k=10 (Fig. 4.6) - enlarged part of the group with the Eriophyidae and part of the Phytoptidae (Fig. 4.9): enlarged part 2F. Black numbers above branches are the character numbers of the homoplasious characters supporting the nodes. Green numbers underneath the branches close to the nodes are the node numbers from TNT. Underlined terminal taxa are included in the 66 taxon data matrix.

Fig. 4.16. The strict consensus of 32 trees found with heuristic parsimony analysis of the 318 taxon x 117 character data matrix, using "new technologies" in TNT, under implied weighting of characters with k=10 (Fig. 4.6) - enlarged part of the group with the Eriophyidae and part of the Phytoptidae (Fig. 4.9): enlarged part 2G. Black numbers above branches are the character numbers of the homoplasious characters supporting the nodes. Green numbers underneath the branches close to the nodes are the node numbers from TNT. Informal names of groups discussed in the text are on the right. Parts of tree blocked in grey also occur, with the same topology, in the estimated consensus tree found from analyzing the 318 taxon data matrix under implied character weighting with k=20 (Fig. 4.26). On the right of terminal taxon names - blue E-numbers are reference numbers for groups found in the estimated consensus tree of the 318 taxon data matrix found under equal character weighting (Fig. 4.5). Underlined terminal taxa are included in the 66 taxon data matrix.

Fig. 4.17. The strict consensus of 32 trees found with heuristic parsimony analysis of the 318 taxon x 117 character data matrix, using "new technologies" in TNT, under implied weighting of characters with k=10 (Fig. 4.6) - enlarged part of the group with the Eriophyidae and part of the Phytoptidae (Fig. 4.9): enlarged part 2H. Black numbers above branches are the character numbers of the homoplasious characters supporting the nodes. Green numbers underneath the branches close to the nodes are the node numbers from TNT. Parts of tree blocked in grey also occur, with the same topology, in the estimated consensus tree found from analyzing the 318 taxon data matrix under implied character weighting with k=20 (Fig. 4.26). On the right of terminal taxon names - blue E-numbers are reference numbers for groups found in the estimated consensus tree found under equal character weighting (Fig. 4.5), blue e-numbers are reference numbers for groups found in strict consensus of most parsimonious trees found for 66 taxon data matrix under equal character weighting (Fig. 4.42). Underlined terminal taxa are included in the 66 taxon data matrix.

Fig. 4.18. The strict consensus of 32 trees found with heuristic parsimony analysis of the 318 taxon x 117 character data matrix, using "new technologies" in TNT, under implied weighting of characters with k=10 (Fig. 4.6) - enlarged part of the group with the Eriophyidae and part of the Phytoptidae (Fig. 4.9): enlarged part 2I. Black numbers above branches are the character numbers of the synapomorphies (encircled in red) or homoplasious characters supporting the nodes. Green numbers underneath the branches close to the nodes are the node numbers from TNT. Informal name of the group discussed in the text is indicated with an arrow. Parts of tree blocked in grey also occur, with the same topology, in the estimated consensus tree found from analyzing the 318 taxon data matrix under implied character weighting with k=20 (Fig. 4.26). On the right of terminal taxon names - blue E-numbers are reference numbers for groups found in the estimated consensus tree of the 318 taxon data matrix found under equal character weighting (Fig. 4.5), blue e-numbers are reference numbers for groups found in strict consensus of most parsimonious trees found for 66 taxon data matrix under equal character weighting (Fig. 4.42). Underlined terminal taxa are included in the 66 taxon data matrix.

Fig. 4.19. The strict consensus of 32 trees found with heuristic parsimony analysis of the 318 taxon x 117 character data matrix, using "new technologies" in TNT, under implied weighting of characters with k=10 (Fig. 4.6): enlarged part of tree at node numbered three in Fig. 4.6, which consists of the Diptilomiopidae clade, to largely show topology. The tree is divided into four parts 3A-3D which are enlarged in Figs 420-4.23.

Fig. 4.20. The strict consensus of 32 trees found with heuristic parsimony analysis of the 318 taxon x 117 character data matrix, using "new technologies" in TNT, under implied weighting of characters with k=10 (Fig. 4.6) - enlarged Diptilomiopidae clade (Fig. 4.19): enlarged part 3A. Black numbers above branches are the character numbers of the synapomorphies (encircled in red) or homoplasious characters supporting the nodes. Green numbers underneath the branches close to the nodes are the node numbers from TNT. Informal names of groups discussed in the text are on the right. The parts of the tree blocked in grey also occur, with the same topology, in the estimated consensus tree found from analyzing the 318 taxon data matrix under implied character weighting with k=20 (Fig. 4.26). The grey blocks with a thick light blue margin connecting them, are one larger group in Fig. 4.26 split up in two smaller groups in the tree above. The taxa included in the area margined by the grey stipple line, are positioned close together in the 318 taxon data matrix analysed under implied character weighting with k=20 (Fig. 4.36), excluding Steopa and including Rhinotergum and Hyborhinus. On the right of terminal taxon names - blue E-numbers are reference numbers for groups found in the estimated consensus tree of the 318 taxon data matrix found under equal character weighting (Fig. 4.5), blue e-numbers are reference numbers for groups found in strict consensus of most parsimonious trees found for the 66 taxon data matrix under equal character weighting (Fig. 4.42). Underlined terminal taxa are included in the 66 taxon data matrix.

Fig. 4.21. The strict consensus of 32 trees found with heuristic parsimony analysis of the 318 taxon x 117 character data matrix, using "new technologies" in TNT, under implied weighting of characters with k=10 (Fig. 4.6) - enlarged Diptilomiopidae clade (Fig. 4.19): enlarged part 3B. Black numbers above branches are the character numbers of the synapomorphies (encircled in red) or homoplasious characters supporting the nodes. Green numbers underneath the branches close to the nodes are the node numbers from TNT. Informal names of groups discussed in the text are on the right. The parts of the tree blocked in grey also occur, with the same topology, in the estimated consensus tree found from analyzing the 318 taxon data matrix under implied character weighting with k=20 (Fig. 4.26). On the right of terminal taxon names - blue E-numbers are reference numbers for groups found in the estimated consensus tree of the 318 taxon data matrix found under equal character weighting (Fig. 4.5), blue e-numbers are reference numbers for groups found in the strict consensus of most parsimonious trees found for the 66 taxon data matrix under equal character weighting (Fig. 4.42), the red 66D indicates those taxa which are part of a clade at node 118 (Fig. 4.45) supported by two synapomorphies in the strict consensus of most parsimonious trees found for the 66 taxon data matrix under implied character weighting with k=999 (Fig. 4.43), the taxa marked with the blue cross are part of the One-Diptilomiopinae group (polytomy) in the estimated consensus tree found from analyzing the 318 taxon data matrix under implied character weighting with k=20 (Fig. 4.37). Underlined terminal taxa are included in the 66 taxon data matrix.

Fig. 4.22. The strict consensus of 32 trees found with heuristic parsimony analysis of the 318 taxon x 117 character data matrix, using "new technologies" in TNT, under implied weighting of characters with k=10 (Fig. 4.6) - enlarged Diptilomiopidae clade (Fig. 4.19): enlarged part 3C. Black numbers above branches are the character numbers of homoplasies supporting the nodes. Green numbers underneath the branches close to the nodes are the node numbers from TNT. Informal names of groups discussed in the text are on the right. The parts of the tree blocked in grey also occur, with the same topology, in the estimated consensus tree found from analyzing the 318 taxon data matrix under implied character weighting with k=20 (Fig. 4.26). On the right of terminal taxon names - blue E-numbers are reference numbers for groups found in the estimated consensus tree of the 318 taxon data matrix found under equal character weighting (Fig. 4.5), blue e-numbers are reference numbers for groups found in the strict consensus of most parsimonious trees found for the 66 taxon data matrix under equal character weighting (Fig. 4.42), the red 66D indicates those taxa which are part of a clade at node 118 (Fig. 4.45) supported by two synapomorphies in the strict consensus of most parsimonious trees found for the 66 taxon data matrix under implied character weighting with k=999 (Fig. 4.43), the taxa marked with the blue cross are part of the One-Diptilomiopinae group (polytomy) in the estimated consensus tree found from analyzing the 318 taxon data matrix under implied character weighting with k=20 (Fig. 4.37). Underlined terminal taxa are included in the 66 taxon data matrix.

Fig. 4.23. The strict consensus of 32 trees found with heuristic parsimony analysis of the 318 taxon x 117 character data matrix, using "new technologies" in TNT, under implied weighting of characters with k=10 (Fig. 4.6) - enlarged Diptilomiopidae clade (Fig. 4.19): enlarged part 3D. Black numbers above branches are the character numbers of the synapomorphies (encircled in red) or homoplasious characters supporting the nodes. Green numbers underneath the branches close to the nodes are the node numbers from TNT. Informal names of groups discussed in the text are on the right. The parts of the tree blocked in grey also occur, with the same topology, in the estimated consensus tree found from analyzing the 318 taxon data matrix under implied character weighting with k=20 (Fig. 4.26). On the right of terminal taxon names - blue E-numbers are reference numbers for groups found in the estimated consensus tree of the 318 taxon data matrix found under equal character weighting (Fig. 4.5), blue e-numbers are reference numbers for groups found in the strict consensus of most parsimonious trees found for the 66 taxon data matrix under equal character weighting (Fig. 4.42), the red 66D indicates those taxa which are part of a clade at node 118 (Fig. 4.45) supported by two synapomorphies in the strict consensus of most parsimonious trees found for the 66 taxon data matrix under implied character weighting with k=999 (Fig. 4.43). Underlined terminal taxa are included in the 66 taxon data matrix.

Fig. 4.24. Symmetric resample absolute group frequency (GF) values of symmetric resampling (P=33) of the 318 taxon data matrix, done in TNT with heuristic ("traditional" in TNT) search under implied weighting of characters with k=10, with 1000 replicates, cut at 50. Values are given above branches. Only those groupings which were not collapsed are presented, the taxa with unresolved relationships and the collapsed groups are substituted by the thick vertical bar.

Fig. 4.25. Symmetric resample group frequency differences (GC) values of symmetric resampling (P=33) of the 318 taxon data matrix done in TNT with heuristic ("traditional" in TNT) search under implied weighting of characters with k=10, with 1000 replicates, cut at 20. Values are given above branches. The resolved part of the tree with groups (supported by GC values of 20 or above) which did not collapse is enlarged on the right hand side.

Fig. 4.26. Estimated consensus tree found with the analysis of the 318 taxon x 117 character data matrix under implied character weighting with k=20 in TNT. Total fit = 94.47; Adjusted homoplasy = 35.53; Total length = 2970; CI = 0.101; RI = 0.521; Nodes = 103. Uninformative characters were included. Unsupported branches were not collapsed. The entire tree is presented to show topology, and it is a metric tree. Tree presented from TNT. Tree name is 318tax-k20 tree. The bars on the right hand side indicate families and some notes on broad groupings and clades. The red bar and text = Phytoptidae, the green bar and text = Eriophyidae and the blue bar and text = Diptilomiopidae. Although the bar indicates subdivisions within families, and largely relationships between them, it doesn't always indicate relationships between the groups correctly, and also not necessarily indicate the order in which the groups occur in the tree, because groups or taxa at one node, or groups in a polytomy do not have "polarity" or "order" and can rotate around the node.

Fig. 4.27. Estimated consensus tree found with the analysis of the 318 taxon x 117 character data matrix under implied character weighting with k=20 (318tax-k20 tree, Fig. 4.26): enlarged part of tree including outgroup species and branch of node with the Eriophyoidea clade. Black numbers above branches are the character numbers of the synapomorphies or homoplasious characters supporting the nodes. The node numbers from TNT are the green numbers underneath the branches and close to the nodes.

Fig. 4.28. Estimated consensus tree found with the analysis of the 318 taxon x 117 character data matrix under implied character weighting with k=20 (318tax-k20 tree, Fig. 4.26): detail of basal part of tree enlarged; the group at node 320 divided into smaller groups (Groups 1-16, and the Diptilomiopidae clade) which are enlarged in Figs 4.29-4.35. Black numbers above branches are the character numbers of the homoplasious characters supporting the nodes. The node numbers from TNT are the green numbers underneath the branches and close to the nodes. Informal names of groups discussed in the text are on the right.

Fig. 4.29. Estimated consensus tree found with the analysis of the 318 taxon x 117 character data matrix under implied character weighting with k=20 (318tax-k20 tree, Fig. 4.26): enlarged view of the polytomy of species with relationships between them unresolved and which are part of the group at node 320 (Fig. 4.28). Black numbers above the branches are the character numbers of the homoplasious characters supporting the terminal taxa.

Fig. 4.30. Estimated consensus tree found with the analysis of the 318 taxon x 117 character data matrix under implied character weighting with k=20 (318tax-k20 tree, Fig. 4.26): enlarged Groups 1-5 of Fig. 4.28, and corrected Group 5. Black numbers above branches are the character numbers of the homoplasious characters supporting the nodes. The pink number marked with * on the branch of node 400 of Group 5 is the number of a character in the 318 taxon matrix that were accidentily wrongly coded for *Thamnacus rhamnicola* and *Trimeracarus heptapleuri* as 5 (shape of empodium on leg I divided); it should have been coded as 1 (shape of empodium simple). The data was corrected, and the estimated consensus under implied character weighting with k = 20, here presented, was re-analysed. In the tree with Character 103 coded wrongly, *Thamnacus* groups with *Trimeracarus* and *Diphytoptus*, partly supported by the empodium being divided (Character 103), and *Tegoprionus* and *Monotrymacus* are in the polytomy of this tree, in the tree of the corrected data, *Thamnacus* groups with *Tegoprionus* and *Monotrymacus*, and *Trimeracarus* and *Diphytoptus* are in the polytomy. The node numbers from TNT are the green numbers underneath the branches and close to the nodes.

Fig. 4.31. Estimated consensus tree found with the analysis of the 318 taxon x 117 character data matrix under implied character weighting with k=20 (318tax-k20 tree, Fig. 4.26): enlarged Groups 6-9 of Fig. 4.28. Black numbers above branches are the character numbers of the homoplasious characters supporting the nodes. The node numbers from TNT are the green numbers underneath the branches and close to the nodes.

Fig. 4.32. Estimated consensus tree found with the analysis of the 318 taxon x 117 character data matrix under implied character weighting with k=20 (318tax-k20 tree, Fig. 4.26): enlarged Groups 10-11 of Fig. 4.28. Black numbers above branches are the character numbers of the homoplasious characters supporting the nodes. The node numbers from TNT are the green numbers underneath the branches and close to the nodes. Informal names of groups discussed in the text are on the right.

Fig. 4.33. Estimated consensus tree found with the analysis of the 318 taxon x 117 character data matrix under implied character weighting with k=20 (318tax-k20 tree, Fig. 4.26): enlarged Groups 13-14 of Fig. 4.28. Black numbers above branches are the character numbers of the homoplasious characters supporting the nodes. The node numbers from TNT are the green numbers underneath the branches and close to the nodes. Informal names of groups discussed in the text are on the right, and some indicated with arrows.

Fig. 4.34. Estimated consensus tree found with the analysis of the 318 taxon x 117 character data matrix under implied character weighting with k=20 (318tax-k20 tree, Fig. 4.26): enlarged Groups 15-16 of Fig. 4.28. Black numbers above branches are the character numbers of the homoplasious characters supporting the nodes. The node numbers from TNT are the green numbers underneath the branches and close to the nodes. Informal names of groups discussed in the text are on the right, and some indicated with arrows.

Fig. 4.35. Estimated consensus tree found with the analysis of the 318 taxon x 117 character data matrix under implied character weighting with k=20 (318tax-k20 tree, Fig. 4.26): enlarged Group 17 (Diptilomiopidae clade) of Fig. 4.28. The clade in this figure and at this enlargement is largely presented to show topology and to divide the clade into four separate parts (Diptilomiopidae 17.1-17.4) which are enlarged in Figs 4.36-4.39. Black numbers above branches are the character numbers of the homoplasious characters supporting the nodes. Informal names of groups discussed in the text are on the right.

Fig. 4.36. Estimated consensus tree found with the analysis of the 318 taxon x 117 character data matrix under implied character weighting with k=20 (318tax-k20 tree, Fig. 4.26), enlarged Group 17 (Diptilomiopidae clade) (Fig. 4.35): enlarged group Diptilomiopidae 17.1. Black numbers above branches are the character numbers of the homoplasious characters supporting the nodes. The node numbers from TNT are the green numbers underneath the branches and close to the nodes. Informal names of groups discussed in the text are on the right.

Fig. 4.37. Estimated consensus tree found with the analysis of the 318 taxon x 117 character data matrix under implied character weighting with k=20 (318tax-k20 tree, Fig. 4.26), enlarged Group 17 (Diptilomiopidae clade) (Fig. 4.35): enlarged group Diptilomiopidae 17.2. Black numbers above branches are the character numbers of the homoplasious characters supporting the nodes. The node numbers from TNT are the green numbers underneath the branches and close to the nodes. The species marked with the blue crosses are part constitute the One-Diptilomiopinae group, and the blue crosses are mapped next to the same species in the 318tax-k10 tree (Figs 4.21-4.22). Informal name of group discussed in the text is on the right.

Fig. 4.38. Estimated consensus tree found with the analysis of the 318 taxon x 117 character data matrix under implied character weighting with k=20 (318tax-k20 tree, Fig. 4.26), enlarged Group 17 (Diptilomiopidae clade) (Fig. 4.35): enlarged group Diptilomiopidae 17.3, which is a polytomy that is part of the group at node 378. Black numbers above branches are the character numbers of the homoplasious characters supporting the nodes. The node number from TNT is the green number underneath the branch and close to the node.

Fig. 4.39. Estimated consensus tree found with the analysis of the 318 taxon x 117 character data matrix under implied character weighting with k=20 (318tax-k20 tree, Fig. 4.26), enlarged Group 17 (Diptilomiopidae clade) (Fig. 4.35): enlarged group Diptilomiopidae 17.4. Black numbers above branches are the character numbers of the homoplasious characters supporting the nodes. The node numbers from TNT are the green numbers underneath the branches and close to the nodes. Informal names of groups discussed in the text are on the right.

Figure 4.40. Summary (318-summary tree) of the 318tax-k10 tree (Fig. 4.6), constructed manually to schematically reflect the broad relationships between taxa from the 318 taxon data set which were included in the 66 taxon data set. It is a non-metric tree. It was literally done by eliminating those taxa not included in the 66 taxon analyses from the 318tax-k10 tree (Figs 4.6-4.23). The tree does not portray and should not be interpreted as literally sister group relationships found in the 318tax-k10 tree, but rather relative relationships and a hypothetical topology of what the topology of a 66 taxon tree in this study would be if it fully supported the relative relationships between taxa found in the 318tax-k10 tree. Parts of the tree blocked in grey also occur, with the same topology, in the 66tax-k999 tree (Fig. 4.43); parts of the tree blocked in stippled line block occur in the 66tax-k999 tree, but with different topologies.

Fig. 4.41. Strict consensus (Total fit = 38.91; Adjusted homoplasy = 47.09; Total length = 942; CI = 0.201; RI = 0.181) of 768 most parsimonious trees (each - Total fit = 44.20; Adjusted homoplasy = 41.80; Total length = 648; CI = 0.292; RI = 0.501) found with heuristic parsimony analysis of the 66 taxon x 60 character data matrix, using “traditional searches” in TNT, with the best score hit 207 times out of 7000 (replications overflowed), under equal character weights. Uninformative characters were excluded. Tree plotted with Winclada. The entire tree is presented to show topology, and it is a metric tree. Tree name is 66taxEq tree. The resolved part of the tree is enlarged in Fig. 4.42. Open circles are homoplasies, black circles synapomorphies and orange circles character states which are not interrupted (not “homoplasious”). Character numbers above, and character states below circles.

Fig. 4.42. Strict consensus of 768 most parsimonious trees found with heuristic parsimony analysis of the 66 taxon x 60 character data matrix, using "traditional searches" in TNT under equal character weights (66taxEq tree, Fig. 4.41): enlarged resolved part of the Eriophyoidea clade. Open circles are homoplasies, black circles synapomorphies and orange circles character states which are not interrupted (not "homoplasious"). Character numbers above, and character state numbers below circles. The node numbers from TNT are the green numbers on the nodes. Blue e-numbers on left are reference numbers for groups found in tree, for indication of the groups on other trees. Informal names of groups discussed in text are on the right.

Fig. 4.43. Strict consensus (Total fit = 85.54; Adjusted homoplasy = 0.45; Total length = 649; CI = 0.291; RI = 0.501) of 3 most parsimonious trees (each - Total fit = 85.55; Adjusted homoplasy = 0.45; Total length = 648; CI = 0.292; RI = 0.501) found with heuristic parsimony analysis of the 66 taxon x 60 character data matrix, using "traditional searches" in TNT, with the best score hit 15 times out of 7000, 3 trees swapped with TBR branch-swapping, same 3 trees found, under implied character weighting with k=999, k=500, k=100, k=80, k=50 and k=40. Uninformative characters were excluded. Unsupported nodes were collapsed. Tree plotted with Winclada. The entire tree is presented to show topology, and it is a metric tree. Tree name is 66tax-k999 tree. The bar on the right hand side indicate families and some notes on broad groupings. The red bar and text = Phytoptidae, the green bar and text = Eriophyidae and the blue bar and text = Diptilomiopidae. Although the bar indicates subdivisions within families, and largely relationships between the, it does not always indicate relationships between the groups correctly, and also not necessarily indicate the order in which the groups occur in the tree, because groups or taxa at one node do not have "polarity" or "order" and can rotate around the node. The parts of the tree blocked in grey also occur, with the same topology, in the 66tax-k30 tree (Fig. 4.51) which is one tree found with heuristic searches of the 66 taxon data matrix under implied character weighting with k=30. The tree is divided into six parts, which are enlarged in Figs 4.44-4.48.

Fig. 4.44 Part A. Strict consensus of 3 most parsimonious trees found with heuristic parsimony analysis of the 66 taxon x 60 character data matrix, using "traditional searches" in TNT under implied weighting of character with k=999, k=500, k=100, k=80, k=50 and k=40 (66tax-k999 tree, Fig. 4.43): enlarged Part A. Unsupported nodes were collapsed. Open circles are homoplasies, black circles synapomorphies and orange circles character states which are not interrupted (not "homoplasious"). Character numbers above, and character state numbers below circles. The node numbers from TNT are the green numbers on the nodes.

Fig. 4.44 Part B. Strict consensus of 3 most parsimonious trees found with heuristic parsimony analysis of the 66 taxon x 60 character data matrix, using "traditional searches" in TNT under implied weighting of character with k=999, k=500, k=100, k=80, k=50 and k=40 (66tax-k999 tree, Fig. 4.43): enlarged Part B. Unsupported nodes were collapsed. Open circles are homoplasies, black circles synapomorphies and orange circles character states which are not interrupted (not "homoplasious"). Character numbers above, and character state numbers below circles. The node numbers from TNT are the green numbers on the nodes. Informal names of groups discussed in the text are on the right. Blue e-numbers on the right of terminal taxon names are reference numbers for groups found in the strict consensus of most parsimonious trees found for the 66 taxon data matrix under equal character weights (Fig. 4.42).

Fig. 4.45. Strict consensus of 3 most parsimonious trees found with heuristic parsimony analysis of the 66 taxon x 60 character data matrix, using "traditional searches" in TNT under implied weighting of character with k=999, k=500, k=100, k=80, k=50 and k=40 (66tax-k999 tree, Fig. 4.43): enlarged Part C. Unsupported nodes were collapsed. Open circles are homoplasies, black circles synapomorphies and orange circles character states which are not interrupted (not "homoplasious"). Character numbers above, and character state numbers below circles. The node numbers from TNT are the green numbers on the nodes. Informal names of groups discussed in the text are on the right. Blue e-numbers on the right of terminal taxon names are reference numbers for groups found in the strict consensus of most parsimonious trees found for the 66 taxon data matrix under equal character weights (Fig. 4.42).

Fig. 4.46. Strict consensus of 3 most parsimonious trees found with heuristic parsimony analysis of the 66 taxon x 60 character data matrix, using "traditional searches" in TNT under implied weighting of character with k=999, k=500, k=100, k=80, k=50 and k=40 (66tax-k999 tree, Fig. 4.43): enlarged Part D. Unsupported nodes were collapsed. Open circles are homoplasies, black circle an autapomorphy and orange circles character states which are not interrupted (not "homoplasious"). Character numbers above, and character state numbers below circles. The node numbers from TNT are the green numbers on the nodes. Informal names of groups discussed in the text are on the right. Blue e-numbers on the right of terminal taxon names are reference numbers for groups found in the strict consensus of most parsimonious trees found for the 66 taxon data matrix under equal character weights (Fig. 4.42).

Fig. 4.47. Strict consensus of 3 most parsimonious trees found with heuristic parsimony analysis of the 66 taxon x 60 character data matrix, using "traditional searches" in TNT under implied weighting of character with k=999, k=500, k=100, k=80, k=50 and k=40 (66tax-k999 tree, Fig. 4.43): enlarged Part E. Unsupported nodes were collapsed. Open circles are homoplasies and orange circles character states which are not interrupted (not "homoplasious"). Character numbers above, and character state numbers below circles. The node numbers from TNT are the green numbers on the nodes. Informal names of groups discussed in the text are on the right. Blue e-numbers on the right of terminal taxon names are reference numbers for groups found in the strict consensus of most parsimonious trees found for the 66 taxon data matrix under equal character weights (Fig. 4.42).

Fig. 4.48. Strict consensus of 3 most parsimonious trees found with heuristic parsimony analysis of the 66 taxon x 60 character data matrix, using "traditional searches" in TNT under implied weighting of character with k=999, k=500, k=100, k=80, k=50 and k=40 (66tax-k999 tree, Fig. 4.43): enlarged Part F. Unsupported nodes were collapsed. Open circles are homoplasies, black circles synapomorphies and orange circles character states which are not interrupted (not "homoplasious"). Character numbers above, and character state numbers below circles. The node numbers from TNT are the green numbers on the nodes. Informal names of groups discussed in the text are on the right. Blue e-numbers on the right of terminal taxon names are reference numbers for groups found in the strict consensus of most parsimonious trees found for the 66 taxon data matrix under equal character weights (Fig. 4.42).

Figure 4.49. Symmetric resample absolute group frequency (GF) values of symmetric resampling (P=33) of the 66 taxon x 60 character data matrix done in TNT with heuristic ("traditional" in TNT) searches under implied character weighting with k=999, with 1000 replicates, cut at 50. Values are given above branches.

Figure 4.50. Symmetric resample group frequency difference (GC) values of symmetric resampling (P=33) of the 66 taxon x 60 character data matrix done in TNT with heuristic ("traditional" in TNT) searches under implied character weighting with k=999, with 1000 replicates, cut at 1. Only values of 20 or above were regarded as significant, and the other nodes were regarded as unsupported. Values are given above branches.

Fig. 4.51. One most parsimonious tree (Total fit = 74.68; Adjusted homoplasy = 11.32; Total length = 651; CI = 0.290; RI = 0.497) found with heuristic parsimony analysis of the 66 taxon x 60 character data matrix, using "traditional searches" in TNT, with the best score hit 2 times out of 7000, under implied character weighting with k=30. Uninformative characters were excluded. Unsupported nodes were collapsed. Tree plotted with Winclada. The entire tree is presented to show topology, and it is a metric tree. Tree name is 66tax-k30 tree. The parts of the tree blocked in grey also occur, with the same topology, in the 66tax-k999 tree (Fig. 4.43) which is a strict consensus tree of 3 most parsimonious trees found with heuristic search under implied character weighting of k=999. Only the two parts of the tree (Parts A and B) which partly differ in topology are enlarged in Figs 4.52 and 4.53 respectively.

Fig. 4.52. One most parsimonious tree found with heuristic parsimony analysis of the 66 taxon x 60 character data matrix, using "traditional searches" in TNT under implied character weighting with k=30 (66tax-k30 tree, Fig. 4.51): enlarged Part A. Unsupported nodes were collapsed. The parts of the tree blocked in grey also occur, with the same topology, in the 66tax-k999 tree (Fig. 4.43) which is a strict consensus tree of 3 most parsimonious trees found with heuristic search under implied character weighting of k=999. Open circles are homoplasies, black circles synapomorphies and orange circles character states which are not interrupted (not "homoplasious"). Character numbers above, and character state numbers below circles. The node numbers from TNT are the green numbers on the nodes. Informal names of groups discussed in the text are on the right.

Fig. 4.53. One most parsimonious tree found with heuristic parsimony analysis of the 66 taxon x 60 character data matrix, using "traditional searches" in TNT under implied character weighting with k=30 (66tax-k30 tree, Fig. 4.51): enlarged Part B. Unsupported nodes were collapsed. The parts of the tree blocked in grey also occur, with the same topology, in the 66tax-k999 tree (Fig. 4.43) which is a strict consensus tree of 3 most parsimonious trees found with heuristic search under implied character weighting of k=999. Open circles are homoplasies, black circles synapomorphies and orange circles character states which are not interrupted (not "homoplasious"). Character numbers above, and character state numbers below circles. The node numbers from TNT are the green numbers on the nodes. Informal names of groups discussed in the text are on the right.

Fig. 4.54. One most parsimonious tree (Total fit = 70.86; Adjusted homoplasy = 15.14; Total length = 659; CI = 0.287; RI = 0.489) found with heuristic parsimony analysis of the 66 taxon x 60 character data matrix, using "traditional searches" in TNT, with the best score hit 1 time out of 7000, under implied character weighting with k=20. Uninformative characters were excluded. Unsupported nodes were collapsed. Tree plotted with Winclada. The entire tree is presented to show topology, and it is a metric tree. Tree name is 66tax-k20 tree. The parts of the tree blocked in grey also occur, with the same topology, in the 66tax-k999 tree (Fig. 4.43) which is a strict consensus tree of 3 most parsimonious trees found with heuristic search under implied character weighting of k=999. This tree is presented, although it is not the preferred tree, because it has an alternative topology to the other two trees presented, and seems to provide useful alternative hypotheses to be investigated. It provides another parameter "test" for the robustness of groups found in other trees, and gives an indication of the change in topology when weighting against homoplasy is slightly more significant than k=999 and 30 which have topologies very similar to one of the most parsimonious trees found under equal weighting. This tree is not discussed in such detail in the text than the other presented trees.

Fig. 4. 55. Corrected data matrix of Hong & Zhang (1996a) using taxa (but taxa are exemplar species, and not genera) characters and character states as defined by Hong & Zhang (1996a). I.) Preferred tree, implied weighting with k=999, implicit enumeration search resulted in one tree with L=85, ci=0.459, ri=0.483. Uninformative characters included, white circles homoplasy, black circles characters without any homoplasy, orange circles character state not interrupted (not homoplasious). Unsupported nodes collapsed. Character numbers above, and character states below branches. Tree search in TNT, tree plotted with Winclada. II.) strict consensus (L=118, ci=0.331, ri=0.112) of 141 trees (each L=85, ci=0.459, ri=0.483), same data as for tree I above, analysed with implicit enumeration in TNT under equal weighting of characters. . The bars on the right hand side of the trees indicate families and other taxa. The red bars and text = Phytoptidae, the green bars and text = Eriophyidae, the blue bars and text = Diptilomiopidae and the gray bar and text = mixture of Eriophyidae and Phytoptidae species. Although the bars indicates subdivisions of families, and largely relationships between them, it doesn't always indicate the order in which the groups occur in the tree, because groups or taxa at one node, or groups in a polytomy do not have "polarity" or "order" and can rotate around the node.

Fig.4.56. Symmetric resampling (P=33) with heuristic (”traditional” in TNT) searches of corrected Hong & Zhang (1996a) data set, 5000 replicates, done under implied weighting of characters with k=999 in TNT: a) group frequencies given above branches, branches with group frequency values of less than 50 are collapsed, average group support of 11; b) frequency differences (GC values) given above branches, branches with group frequency values of less than 1 are collapsed, average group support of 17.3.

Fig. 4.57. Corrected data of Hong & Zhang (1996a) using characters and character states as defined by Hong & Zhang (1996a). Strict consensus (L=87, ci=0.448, ri=0.461) of 2 trees (each L=86, ci=0.453, ri=0.472), analysed with implicit enumeration in TNT under implied weighting of characters with k=3. Uninformative characters included, white circles homoplasy, black circles characters without any homoplasy, orange circles character state not interrupted (not homoplasious). Unsupported nodes collapsed. Character numbers above, and character states below branches. Tree search in TNT, tree plotted with Winclada. The bars on the right hand side of the tree indicate families and other taxa. The red bars and text = Phytoptidae, the green bars and text = Eriophyidae, and the blue bars and text = Diptilomiopidae. Although the bars indicates subdivisions of families, and largely relationships between them, it doesn't always indicate the order in which the groups occur in the tree, because groups or taxa at one node, or groups in a polytomy do not have “polarity” or “order” and can rotate around the node.

Fig. 4.58. Corrected data of Hong & Zhang (1996a) using characters and character states similar to the present analyses. I.) Strict consensus (L=132, ci=0.576, ri=0.309) of 10 trees (each L=117, ci=0.650, ri=0.494), analysed under equal weighting; II.) strict consensus (L=118, ci=0.644, ri=0.481) of 3 trees (each L=117, ci=0.650, ri=0.494) (a subcollection of 10 trees obtained under equal weighting). Data analysed with implicit enumeration in TNT under equal character weights. Uninformative characters included, white circles homoplasy, black circles characters without any homoplasy, orange circles character state not interrupted (state not homoplasious). Unsupported nodes collapsed. Character numbers above, and character states below branches. Tree search in TNT, tree plotted with Winclada. The bars on the right hand side of the tree indicate families and other taxa. The red bars and text = Phytoptidae, the green bars and text = Eriophyidae, the blue bars and text = Diptilomiopidae, and the gray bar and text = a mixture of species of the Phytoptidae and Eriophyidae. Although the bars indicates subdivisions of families, and largely relationships between them, it doesn't always indicate the order in which the groups occur in the tree, because groups or taxa at one node, or groups in a polytomy do not have “polarity” or “order” and can rotate around the node.

Fig. 4.59. Corrected data of Hong & Zhang (1996a) using characters and character states similar to the present analyses. Strict consensus (L=118, ci=0.644, ri=0.481) of 3 trees (each L=117, ci=0.650, ri=0.494), under implied weighting, k=100). Data analysed with implicit enumeration in TNT under equal character weights. Uninformative characters included, white circles homoplasy, black circles characters without any homoplasy, orange circles character state not interrupted (state not homoplasious). Unsupported nodes collapsed. Character numbers above, and character states below branches. Tree search in TNT, tree plotted with Winclada. The bars on the right hand side of the tree indicate families and other taxa. The red bars and text = Phytoptidae, the green bars and text = Eriophyidae, and the blue bars and text = Diptilomiopidae. Although the bars indicates subdivisions of families, and largely relationships between them, it doesn't always indicate the order in which the groups occur in the tree, because groups or taxa at one node, or groups in a polytomy do not have “polarity” or “order” and can rotate around the node.

Fig. 4.60. Corrected data of Hong & Zhang (1996a) using characters and character states similar to the present analyses. Strict consensus (L=118, ci=0.644, ri=0.481) of 3 trees (each L=117, ci=0.650, ri=0.494), under implied weighting, k=100). Data analysed with implicit enumeration in TNT under equal character weights. Uninformative characters included, white circles homoplasy, black circles characters without any homoplasy, orange circles character state not interrupted (state not homoplasious). Unsupported nodes collapsed. Character numbers above, and character states below branches. Tree search in TNT, tree plotted with Winclada. The bars on the right hand side of the tree indicate families and other taxa. The red bars and text = Phytoptidae, the green bars and text = Eriophyidae, and the blue bars and text = Diptilomiopidae. Although the bars indicates subdivisions of families, and largely relationships between them, it doesn't always indicate the order in which the groups occur in the tree, because groups or taxa at one node, or groups in a polytomy do not have “polarity” or “order” and can rotate around the node.

Fig.4.61. Symmetric resampling (P=33) with heuristic (”traditional” in TNT) searches of corrected Hong & Zhang (1996a) data set, with modified character states (this study), 5000 replicates, done under implied weighting of characters with k=100 in TNT: a) group frequencies given above branches, branches with group frequency values of less than 50 are collapsed, average group support of 10; b) frequency differences (GC values) given above branches, branches with group frequency values of less than 1 are collapsed, average group support of 15.

Fig. 4.62. Corrected data of Hong & Zhang (1996a) using characters and character states similar to the present analyses. One tree (L=118, ci=0.644, ri=0.481) resulted from implicit enumeration search in TNT under implied weighting, k=3. Data analysed with implicit enumeration in TNT under equal character weights. Uninformative characters included, white circles homoplasy, black circles characters without any homoplasy, orange circles character state not interrupted (state not homoplasious). Unsupported nodes collapsed. Character numbers above, and character states below branches. Tree search in TNT, tree plotted with Winclada. The bars on the right hand side of the tree indicate families and other taxa. The red bars and text = Phytoptidae, the green bars and text = Eriophyidae, and the blue bars and text = Diptilomiopidae. Although the bars indicates subdivisions of families, and largely relationships between them, it doesn't always indicate the order in which the groups occur in the tree, because groups or taxa at one node, or groups in a polytomy do not have “polarity” or “order” and can rotate around the node.

LIST OF TABLES

PROLOGUE

CHAPTER 1

CHAPTER 3

CHAPTER 4

Table 4.2. Tree statistics for estimated consensus trees of 318 taxon data matrix found under different weighting schemes, and for the 32 most parsimonious trees and the strict consensus (Fig. 4.) of these trees found with New Technology Searches in TNT under implied weighting of characters with k = 10. The statistics of the trees that are presented in the results are in bold.

Table 4.3. Tree statistics for most parsimonious (MP) and strict consensus trees of the 66 taxon data matrix found under different weighting schemes. The statistics of the trees that are presented in the results are in bold.

Table 4.4. Re-analysis of the original data matrix of Hong & Zhang (1996a) without any changes to original published data; all characters ordered (similar to original analyses by Hong & Zhang, 1996a). Tree search with implicit enumeration algorithm in TNT. * Uninformative characters included; ** uninformative characters excluded; ◆ rounded to 51 and 47 respectively in WinClada.

Table 4.5. Re-analysis of the corrected scoring of the original data matrix of Hong & Zhang (1996a); Character 32 (length of setae *sc*) ordered, remaining characters unordered. Characters and states as defined and used by Hong & Zhang (1996a). Tree search with implicit enumeration algorithm in TNT. * Uninformative characters included (statistics from TNT); ** uninformative characters excluded (statistics from WinClada); ◆ truncated to 45 (for 0.459), 44 (for 0.448), 0.42 (for 0.427), 0.41 (for 0.419) in WinClada.

Table 4.6. Trees found for the 18 taxon data set with characters included in the data matrix of Hong & Zhang (1996a) but which were corrected and modified to resemble, and be a sub-sample of those characters used for the 318tax and 66tax data sets. Character 32 (length of setae *sc*) ordered, remaining characters unordered. Tree search was done with the implicit enumeration algorithm in TNT. * Uninformative characters included (statistics from TNT); ** uninformative characters excluded (statistics from WinClada); ◆ 0.64 (TNT 0.650), 0.57 (TNT 0.576), 0.41 (TNT 0.420) in WinClada.

Table 4.7. Character consistency indices (ci) and character retention indices (ri) of characters of the estimated consensus tree, found in TNT, of the 318 taxon data matrix under equal character weighting (Fig. 4.3, 4.4.). The indices in light grey are of characters which are uninformative regarding the relationships between ingroup taxa because they are autapomorphic for the Eriophyoidea, or the same for all taxa in the analysis (Characters 7 and 41), the indices within a block with a grey background are those of characters autapomorphic for a terminal ingroup taxon, and the indices in bold and in a block with thickened edges, are of homologous characters.

Table 4.8. Character consistency indices (ci) and retention indices (ri) of characters in the strict consensus of 32 most parsimonious trees found with new technology searches in TNT under implied character weighting with k=10. A total of 117 characters are included in the data matrix, of which 52 are uninformative regarding the relationships between the ingroup (eriophyoid) taxa (the information for characters autapomorphic for the Eriophyoidea, and one character the same for all taxa in the analysis, are in grey, and the cell backgrounds of information for the characters autapomorphic for terminal taxa of the ingroup, are grey). Sixteen of the 65 informative characters are binary characters, and 49 are multistate characters. The number of character states for each character is listed in the column with the heading “state”, 2 is a binary character and M is a multistate character followed by the number of character states. The characters with information in bold, are homologous for this tree.

Table 4.9. Character consistency indices (ci) and character retention indices (ri) of characters of the estimated consensus tree found with the analysis of the 318 taxon data matrix under implied weighting of characters with k=20 in TNT (Fig. 4.26). A total of 117 characters are included in the data matrix, of which 52 are uninformative regarding the relationships between the ingroup (eriophyoid) taxa (ci indices of characters autapomorphic for the Eriophyoidea, and one character the same for all taxa in the analysis are in grey, and the cell backgrounds of the ci indices of

characters autapomorphic for terminal taxa of the ingroup, are grey). The characters with ci indices in bold are homologous for this tree.

Table 4.10. A proposed new classification of suprageneric and genera of the Eriophyoidea, partly based on the phylogeny recovered in the present study. A priority was the preservation of the stability of the classification *sensu* Amrine *et al.* (2003), but with changes based on groups found with phylogenetic analyses in the present study, and which are proposed to render the classification more natural. Drastic changes, particularly to nomenclature and practicality (for classifying and identification), were regarded premature. The proposed classification is thus not entirely phylogenetic, purely based on the phylogeny found in the present study. The relationships and taxonomic positions of the genera are extrapolated from the relationships of the species (usually type species) found in the present study. This essentially assumes the monophyly of genera which is not necessarily true or implied. Where more than one species of a genus were included in the present study, they are included as separate species in the proposed classification. Many *Diptilomiopus* spp. were included in the analyses, but all remain in the Diptilomiopinae, and only the genus name is used.). The genera within a suprageneric taxon are listed alphabetically, and the order in which they are listed does not imply relationships. "*Comb. nov*." refers to the new position of the genus and not to a recombination of the species with another genus. Species and their genera not included in the present study, are not dealt with, and remain classified according to Amrine *et al.* (2003). The classificatory structure and position of the Phyllocoptinae and placement of its genera remain as presented in Amrine *et al.* (2003). Despite the inclusion of their presumably deutogyne females in the present phylogenetic study, *Aceria kenyae* (= *Cisaberoptus kenyae*) and *A. pretoriensis* (= *C. pretoriensis*) are not included in the classification proposed here, and they remain within *Aceria* (Eriophyidae: Eriophyinae) as proposed by Amrine *et al*. (2003).

APPENDIX B

Table B.1. Opisthosomal setae (Figs 3.2, 3.4) (except setae *c1* and *h1*) absent in eriophyoid species included in the present phylogenetic study. Setae *f* and *h2* are never absent in the Eriophyoidea. Only species with at least one of these setae absent are included in the table. Absence of a setal pair is ticked x.

Table B.2. Leg setae (except coxal setae) which are absent in eriophyoid species included in the data set. Where there are more than one species in a genus, only one species was included in the table, or if variation occur between species from the same genus, all such species with different absent setae were included. Only species with some leg setae absent are listed. Absence of a setal pair is ticked with x. Setae *bv* 1 is the seta on the femur of leg I, and *bv* 2 is the seta on the femur of leg II, likewise *l''* 1 is the seta on genu of leg I, and l'' 2 is the seta on genu of leg II. Seta *l'* is the seta on the tibia of leg I, and *ft'* 2 is seta *ft'* on the tarsus of leg II.

Table B.3. List of Eriophyoidea species with wax, including their classification and structures from which the wax is probably secreted, or on which it occurs. The data was obtained from the original descriptions of the mites.

A Considerable Speck

A speck that would have been beneath my sight
On any but a paper sheet so white
Set off across what I had written there.
And I had idly poised my pen in air
To stop it with a period of ink
When something strange about it made me think,
This was no dust speck by my breathing blown,
But unmistakably a living mite
With inclinations it could call its own.
It paused as with suspicion of my pen,
And then came racing wildly on again
To where my manuscript was not yet dry;
Then paused again and either drank or smelt--
With loathing, for again it turned to fly.
Plainly with an intelligence I dealt.
It seemed too tiny to have room for feet,
Yet must have had a set of them complete
To express how much it didn't want to die.
It ran with terror and with cunning crept.
It faltered: I could see it hesitate;
Then in the middle of the open sheet
Cower down in desperation to accept
Whatever I accorded it of fate.
I have none of the tenderer-than-thou
Collectivistic regimenting love
With which the modern world is being swept.
But this poor microscopic item now!
Since it was nothing I knew evil of
I let it lie there till I hope it slept.

I have a mind myself and recognize
Mind when I meet with it in any guise
No one can know how glad I am to find
On any sheet the least display of mind.

-- Robert Frost

Man is certainly crazy. He could not make a mite, yet he makes gods by the dozen.
(Michel E. de Montaigne, 1580)

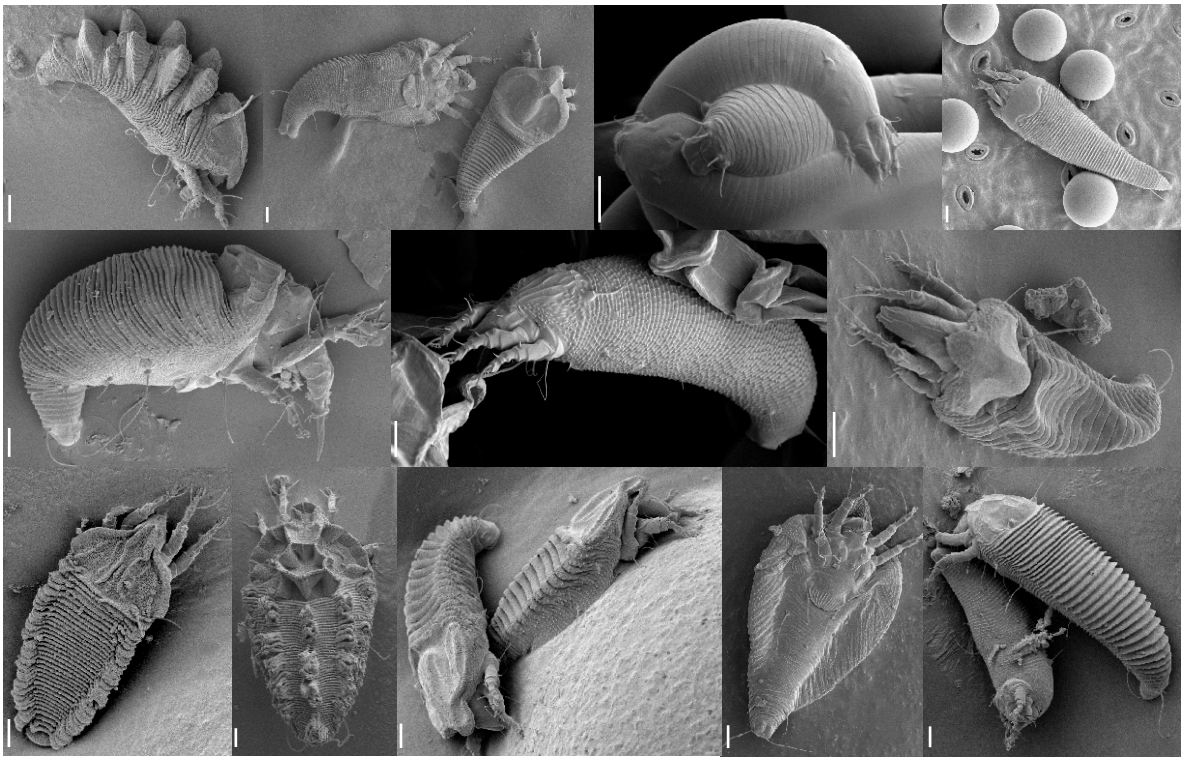

Fig. 0.1. Habitus of mites of the Eriophyoidea: compendium of different genera. Scale bars represent 10μ.

0. PROLOGUE

0.1 ACARI

The Eriophyoidea, which form the subject of this study, are a group of obligatory plant-feeding mites. This superfamily, together with other mites and ticks[1], constitute the subclass Acari (alternative names still in use – Acarina, and in recent years less in use – Acarida). The Acari is one of the largest and most diverse groups of animals (Krantz & Walter, 2009), and rank sixth in animal global diversity after the five largest insect orders (Coleoptera, Hymenoptera, Lepidoptera, Diptera and Hemiptera) (Coddington & Levi, 1991). The word 'mite' originates from Old English and means "a very small creature, beastie or insect", and indeed mites are generally tiny organisms (less than 1 mm long) (Walter & Proctor, 1999). They colonize other living organisms, and virtually every terrestrial, fresh water and marine habitat on earth, including the extreme (Baker & Wharton, 1952; Evans, 1992; Walter & Proctor, 1999; Krantz & Walter, 2009). The omnipresence of mites in the earth's ecosystems is mirrored by the diversity of their habits, including predators, sapro-, phyco- and phytophagous mites, fungivores and parasites of vertebrates and invertebrates (Halliday *et al.*, 1997; Walter & Proctor, 1999; Krantz & Walter, 2009).

Many mites are considered beneficial to humans. Several are predators of undesirable arthropods, some are utilized in controlling weeds (Gerson *et al.*, 2003), while others are major role players in the break-down of soil organic matter (Walter & Proctor, 1999). Mites are also regarded as good indicators of environmental health (Walter & Proctor, 1999).

Mites may also be detrimental to humans. Some species are of medical or veterinary importance, parasitizing either humans directly such as scabies caused by *Sarcoptes scabiei* (Linnaeus, 1758) (Baker, 1999; Walton & Currie, 2007) or their associated animals, such as livestock, pets, poultry, caged birds and honeybees (Baker, 1999). They may infest crops, ornamental plants (Jeppson *et al.*, 1975) as well as cultivated mushrooms (Hughes, 1976; Van der Hoven *et al.*, 1988). These mites can cause severe damage either by their feeding activities or by being vectors of pathogens. Mites can cause hyper-sensitive and allergic reactions by colonizing homes (Hart, 1992), while others tend to infest stored products, and processed foods (Hughes, 1976), and some can interfere with scientific experiments by infesting laboratory insects, plants, animals, or plant cell cultures.

[1] The groups generally known as mites and ticks both belong to the subclass Acari, and ticks can be regarded as "large mites". For convenience, Acari will be generally referred to as "mites" from here on in this dissertation, encompassing the ticks.

The biodiversity of mites is not only varied in habitat, behaviour and life style, but in species richness as well (Krantz & Walter, 2009). In 1997, there were an estimated 48 200 named species of Acari (Halliday *et al.*, 1997), and about 55 000 in 1999 (Walter & Proctor, 1999; Krantz & Walter, 2009), and currently has the largest number of valid described species within the Arachnida (Harvey, 2002). These species are classified into nearly 5 500 genera and 1 200 subgenera representing about 540 families in 124 superfamilies (Krantz & Walter, 2009). The described taxa represent only a scant proportion of mite diversity (Halliday *et al.*, 1997; Walter & Proctor, 1999; Krantz & Walter, 2009), and even those mites living in well-studied biological systems are largely over-looked and unknown (Walter & Proctor, 1999). It is estimated that anywhere between 500 000 to one million mite species may exist, but the total number may be much greater than currently imagined (Krantz, 2009a).

Despite their economic importance and diversity, the study of mites (acarology) remains a largely unexplored discipline (Walter & Proctor, 1999). Historically, the study of mites has for the most part been ignored by zoologists and entomologists alike, probably because mites are not small enough to be handled like protozoans and other pathogens, or soft-bodied enough to be treated as worms, and they are too small to be collected and studied like insects (Baker & Wharton, 1952).

0.2 SYSTEMATICS OF THE ACARI

It is traditionally and generally agreed that terrestrial chelicerate arthropods, including the Acari, are members of the Class Arachnida (Chapter 1, Table 1.1). It is only since the 1990s that cladistic analyses have been utilized to study chelicerate phylogeny (Beall & Labandeira, 1990; Shultz, 1990, 2007; Wheeler & Hayashi, 1998). The systematics of the Chelicerata, and in particular of the Arachnida in the Chelicerata, is still debated and a subject of controversy (Weygoldt, 1998). The Arachnida, however, seems to be a monophyletic taxon, well-supported by morphological characters (Weygoldt, 1998; Shultz, 2007).

The Acari represents one of 11 extant groups (10 orders and one subclass) within the Arachnida (Shultz, 2007). Some of the orders are morphologically easily recognizable, such as the Araneae (spiders), and the Scorpiones (scorpions). Mites, however, are diverse in form and in order to accommodate them in the classification scheme, acarologists treat them as a subclass within the Arachnida (Walter & Proctor, 1999; Krantz & Walter, 2009).

The Acari is among the oldest of all terrestrial animals, with fossils with a moderate level of diversity known from the Early Devonian (about 400 million years ago) (Norton *et al.*, 1988;

Kethley *et al.*, 1989). Krantz (2009b) extrapolated that ancestral mites may have occupied the terrestrial landscape as early as the Late Silurian. Arachnologists and acarologists generally agree that the Acari are a monophyletic group (Lindquist, 1984; Weygoldt, 1998), but some authors (e.g., Van der Hammen, 1977; Alberti, 2000) hypothesized that the group may be diphyletic[2]. Whatever the case, the major lineages within the Acari seem to have originated very early on in the evolution of the Acari and there is substantial morphological divergence within and between them (Lindquist, 1984; Weygoldt, 1998).

It is hypothesized that the Ricinulei is the sister group of the Acari, and they are grouped together as the Acaromorpha (Shultz, 2007). This hypothesis has been tested but is supported by relatively few characters based on cladistic analyses (Weygoldt & Paulus, 1979; Lindquist, 1984; Shultz, 1990, 2007; Evans, 1992).

Leading acarologists divide the Acari either in two (Actinotrichida (Acariformes) and Anactinotrichida (Opilioacarida + Parasitiformes)) (Lindquist, 1984; Evans, 1992), or Acariformes and Parasitiformes at superorder level (Lindquist *et al*., 2009), or three (Acariformes, Opilioacariformes and Parasitiformes) major lineages (Grandjean, 1936; Krantz, 1978; Halliday, 1998; Walter & Proctor, 1999). As exemplified in Table 0.1, the names and taxonomic levels at which these names are used for major groups or lineages within the Acari is widely variable (e.g., Krantz, 1978; Evans, 1992; Walter & Proctor, 1999; Krantz & Walter, 2009) and can be confusing. There has been a remarkable increase in the systematic knowledge on the Acari over the last three decades. Acarine systematics is, however, still based on a fragmentary understanding of the fauna (Krantz & Walter, 2009), and the phylogenies and higher classification within the Acari remains largely unresolved, similar to the situation in the Arthropoda in general (Lindquist *et al*., 2009).

[2] Dunlop & Alberti (2007) reviewed the evidence that supports or contests the monophyly of the Acari.

Table 0.1. The higher classification of the Acari (following Lindquist *et al.*, 2009), with some alternative names and groupings in parentheses, and the taxonomic levels (groups not always used on these levels in the literature) in square brackets. Groups within Acariformes listed to suborder level, Parasitiformes to order level. The groups with phytophagous members are listed (* – some members are phytophagous, ** – all members are obligatory phytophagous) (Lindquist, 1998). It is considered that phytophagy may have developed several times independently in several mite groups (Lindquist, 1998). The Eriophyoidea (subject of this study) and Tetranychoidea (spider mites and their relatives) are the only two groups in which all members and their instars are exclusively and obligatory phytophagous (phytophagous here means to feed on plant sap).

[Superorder] ACARIFORMES (Actinotrichida, Actinochitinosi)

[Orders]

- **Trombidiformes** (Prostigmata)
  [Suborders]
  - **Sphaerolichida**
  - **Prostigmata** (Actinedida + Tarsonemida; Prostigmata suborder (*sensu* Lindquist *et al.*, 2009) or Trombidiformes, + Sphaerolichida). Most diverse mite group in terms of habit, habitat and morphology. Includes free-living predators, fungivores, and parasitic species on plants, vertebrate and invertebrate animals.
    Prostigmatid groups with phytophagous members:

  * Parasitengonina
  * Raphignathoidea
  * Heterostigmatina
  * Eupodoidea
  * Tydeoidea
  ** Tetranychoidea
  ** Eriophyoidea

- **Sarcoptiformes** (Astigmata, Acaridida)
  [Suborders]
  - **Endeostigmata**
  - **Oribatida** (Cryptostigmata, Oribatei). Largely free-living soil inhabiting mites, some live on plants, essentially feeding on dead plant material and fungi, playing an important role in litter-decomposition and soil-formation. Including Cohort **Astigmatina** (Astigmata, Acaridida, Sarcoptiformes) which mostly includes free-living fungivorous and saprophagous mites, often found in large numbers in stored foods and animal nests; also includes the dust mites that are implicated in causing allergies and asthma in humans.
    Only oribatid family with phytophagous species:

  * Galumnidae

[Superorder] PARASITIFORMES
(Anactinotrichida, Parasitiformes + Opilioacariformes, Anactinochitinosi)

[Orders]

- **Holothyrida** (Tetrastigmata). Small group of about 30 relatively large, soil-inhabiting mite species.
- **Ixodida** (Metastigmata). Exclusively blood-feeding ectoparasites of vertebrates (ticks).
- **Mesostigmata** (Gamasida). Typically free-living predators of other small invertebrates in soil, decomposing organic material and on plants, but also include ecto- or endoparasites of vertebrates.
- **Opilioacarida** (Opilioacariformes, Notostigmata). Small group of relatively large mites free-living in dry conditions under stones and in litter.

0.3 ERIOPHYOIDEA

The Eriophyoidea (eriophyoid mites or eriophyoids) are a morphologically distinct group of mites. They are minute (on average 150-250 µm long) with elongated, worm-like and annulated bodies, and are unique in having all instars of both sexes with two pairs of similarly developed legs anteriorly (Fig. 0.1).

0.3.1 Ecology and importance

Eriophyoids generally seek microhabitats on plants in which to live, feed and reproduce. Their mouth-parts are modified to facilitate plant-feeding, and are so small (on average 15-40 µm long) that they can mostly only penetrate epidermal cells, or in the case of some members with slightly longer chelicerae, parenchyma just below the epidermal layer. They feed only on the liquid part of a cell, and cause minimal mechanical damage (Lindquist & Oldfield, 1996; De Lillo & Monfreda, 2004). The feeding of most eriophyoids causes no obvious change in either plant growth or appearance. The feeding of some species, however, may directly induce symptoms, such as a discolouration of tissue (rust), as well as a wide range of growth abnormalities (Fig. 0.2), including gall formation, deformation of growth points, blisters, witches' broom growth and erineum (abnormal plant hair growth) (Jeppson *et al.*, 1975; Westphal & Manson, 1996). These symptoms can occur on all above-ground plant parts, and are probably caused by substances in the mites' saliva being injected into plant cells during feeding (De Lillo & Monfreda, 2004). Symptoms vary in the severity of damage to plants. Based on these symptoms, generally eriophyoid mites are commonly referred to as gall-, rust-, bud-, erineum-, witches' broom- or blister mites, etc. Some eriophyoids are vectors of detrimental plant pathogens, such as viruses and micoplasms (Oldfield & Proeseler, 1996).

Fig. 0.2. Compendium of plant abnormalities caused by feeding of eriophyoid mites. (Photos of symptoms by S. Neser.)

Eriophyoids as a group occur on a vast range of plant families, but the majority of eriophyoid mite species are generally regarded as being very host-specific. Eriophyoidea have a cosmopolitan distribution. They are associated with most groups of land-living multicellular plants.

In southern Africa, 21 eriophyoid species are regarded as economically important agricultural pests (Meyer & Craemer, 1999). The negative economic impact these mites can have on agricultural production, for commercial and subsistence farmers, necessitates a comprehensive knowledge and understanding of their systematics and biology.

The detrimental effect of eriophyoid symptoms can also be useful in agriculture and ecology. Some eriophyoid species are utilised in weed control, especially in classical biological control initiatives, or are investigated as potential weed control agents (Cromroy, 1979; 1984; Craemer, 1993; Gerson *et al.*, 2003; Smith *et al.*, 2010).

Eriophyoid symptoms are easily confused with symptoms from a physiological effect (e.g., dieback of tomato plants caused by the tomato rust mite that may be confused with drought symptoms) or those caused by other organisms, such as pathogens and insects. Thus in many instances the correct control actions for observed damage can not be determined easily. The problem is further exacerbated by the microscopic nature of the mites, and in many cases the lack of knowledge of their presence and on their identity.

Eriophyoids are generally very successful dispersers. They are mainly dispersed by wind (Davis, 1964b; Nault & Styer, 1969; Krantz & Lindquist, 1979; Zhao & Amrine, 1997), but may also be dispersed by insects and other organisms (e.g., Waite & McAlpine, 1992).

0.3.2 Biology

The life cycle of all eriophyoids generally comprises an egg, two nymphal stages, or a larva and nymph, depending on the view of the Acarologist (Shevchenko, 1961; Lindquist, 1996a), and an adult stage (male or female). Sternlicht & Goldenberg (1971) named the stages during the resting period between the first and second nymphs as “nympochrysalis”, and during the period between the second nymph and adult as “imagochrysalis”.

Females are fertilized when they pick up sperm from spermatophores deposited by males (Oldfield *et al.*, 1970; Sternlicht & Goldenberg, 1971). Some eriophyoids were shown to be arrhenotokous (males hatching from haploid or unfertilized eggs, and females from fertilized eggs) (Keifer, 1975a) and this may presumably be true for all eriophyoids.

Some species have an alternation of generations with two different structural types of females, referred to as deuterogyny. The primary female (protogyne) resembles the males and reproduces rapidly during favourable conditions, while the secondary female (deutogyne), with no male counterpart, can carry the species through unfavourable periods (Keifer, 1975a). These alternative forms are of concern to the current classification and identification of eriophyoid mites, and could not be addressed in the present study, but may be of importance to the phylogeny of the group. A more detailed account of deuterogyny in the Eriophyoidea is provided in Chapter 4.